Heat-bath approach to anomalous thermal transport: Effects of inelastic scattering

Zhiqiang Wang [1,*] Rufus Boyack,[2] and K. Levin[1,†]

[1]*Department of Physics and James Franck Institute, University of Chicago, Chicago, Illinois 60637, USA*

[2]*Département de physique, Université de Montréal, Montréal, Québec, Canada H3C 3J7*

(Received 11 January 2022; revised 25 March 2022; accepted 28 March 2022; published 8 April 2022)

We present results for the entire set of anomalous charge and heat transport coefficients for metallic systems in the presence of a finite-temperature heat bath. In realistic physical systems, this necessitates the inclusion of inelastic dissipation mechanisms; relatively little is known theoretically about their effects on anomalous transport. Here we demonstrate how these dissipative processes are strongly intertwined with Berry-curvature physics. Our calculations are made possible by the introduction of a Caldeira-Leggett reservoir, which allows us to avoid the sometimes-problematic device of the pseudogravitational potential. Using our formulas, we focus on the finite-temperature behavior of the important anomalous Wiedemann-Franz ratio. Despite previous expectations, this ratio is found to be nonuniversal as it can exhibit either an upturn or a downturn as temperature increases away from zero. We emphasize that this derives from a *competition* between Berry curvatures having different signs in different regions of the Brillouin zone. We point to experimental support for these observations and for the behavior of an alternative ratio involving a thermoelectric response which, by contrast, appears to be more universal at low temperatures. Our work paves the way for future theory and experiment, demonstrating how inelastic scattering at nonzero temperature affects the behavior of all anomalous transport coefficients.

DOI: 10.1103/PhysRevB.105.134302

I. INTRODUCTION

Charge and thermal transport (both with and without an applied magnetic field) are viewed as providing fundamental information about a condensed matter system. Our understanding of these response properties has recently progressed largely because of the focus on topological quantum materials. Initially, the electrical Hall conductivity was at the heart of this excitement, but attention has now shifted to its thermal analog [1,2]—the thermal Hall conductivity—and to anomalous counterparts of the Nernst and Ettinghausen thermoelectric coefficients [3]. In addition to revelations about topological order [1,4–7], in metallic systems this larger class of thermal and thermoelectric transport contains contributions which derive from Berry-curvature effects [3,8,9] in the underlying band structure. These appear even when the magnetic field is zero; here the associated zero-field response coefficients constitute a class of so-called anomalous transport properties.

These anomalous transport coefficients are the focus of the present paper. They have been well-studied experimentally over the entire range of temperatures [10–12]. Clearly, understanding these finite-temperature transport data requires addressing inelastic dissipation effects, as phonons are always present. It is notable, then, that in the theoretical literature the anomalous Berry-curvature contributions have been restricted [9] to low temperatures, where inelastic processes can be ignored and special connections between the transverse anomalous transport coefficients [such as the Wiedemann-Franz (WF) and Mott relations] obtain [2,3,13].

This paper addresses this shortcoming. We establish what happens to the anomalous charge and heat transport at finite temperatures when inelastic dissipation plays a role, and we focus here on the entire set of transport coefficients. A key finding is our observation that inelastic-scattering properties are strongly intertwined with Berry-curvature physics, as is concretely reflected in the behavior of the transverse WF ratio. We find that the presence of inelastic dissipation can cause this ratio to exhibit an unexpected [11,14] upturn as temperature increases away from zero. This finding appears to be supported by experiments [14]. Central to our paper is the presentation of an alternative methodology for deriving thermal transport coefficients, which avoids many of the ambiguities and pitfalls in more conventional transport schemes. We do so by the introduction of a heat bath such as considered by Caldeira and Leggett [15].

Among the complications in understanding thermal transport is the fact that an applied temperature gradient ∇T represents a statistical rather than a mechanical force; this has led Luttinger [16] to develop an innovative, albeit unintuitive transport framework. Here a gravitational pseudopotential is introduced which gives rise to an effective mechanical force, in analogy with the electric field $\mathbf{E}$ that drives charge transport. This approach builds on Tolman's earlier work [17] demonstrating that addressing transport in curved space-time requires understanding how to treat a position-dependent temperature $T(x)$. [Hereafter, we will omit the spatial dependence of the temperature $T(x)$.] It has, however, been argued to be problematic [18–23], particularly for topological systems. Indeed, lattice effects add an additional complexity, as in this case for the gravitational analog a temperature gradient would correspond to a distorted lattice with spatially dependent hopping.

*zqwang@uchicago.edu
†levin@jfi.uchicago.edu

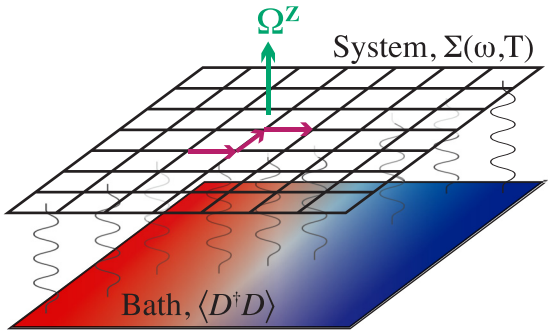

FIG. 1. Schematic diagram of our heat-bath approach. We consider a general multiorbital lattice model of electrons embedded in a heat bath, where the two components are in the same two-dimensional space even though in the diagram they are separated for better visualization. The figure represents the hopping of electrons under the influence of the z component of Berry curvature (dark green vertical arrows with Ω^z). The coupling of the electrons to the heat bath leads to a nonzero dissipation characterized by the electronic self-energy Σ. The equilibrium of the system is maintained through the bath so a correlator for the bath particles, $\langle D^\dagger D\rangle$, is proportional to the Fermi-Dirac distribution at a given local temperature. In thermal transport, a temperature gradient (represented by color changes from red to blue) is applied across the sample to drive a heat current.

A second challenge for computing transverse thermal and thermoelectric transport coefficients comes from the necessity [24] to subtract magnetization heat and charge currents which do not contribute to bulk transport. This subtraction is crucial for the derived transport coefficients to be consistent with the third law of thermodynamics and to satisfy the Onsager reciprocal relations [2,24]. Although the spontaneous charge orbital magnetization [25] in the absence of inelastic scattering is now relatively well established [3,26,27], its heat counterpart is currently still being debated [2,18,28]. Moreover, much less is known about how to incorporate finite-lifetime effects when inelastic scattering is present.

Here we consider a multiorbital system of electrons confined to a lattice embedded in a heat-bath reservoir which serves the dual purpose of maintaining local equilibrium associated with the varying temperatures and establishing the temperature gradients. This system is schematically represented in Fig. 1. The reservoir consists of an infinite number of localized degrees of freedom (electrons in the present case) that can exchange energy and particles with the system. Importantly, a (bilinear) coupling between the system and bath particles gives rise to quantum dissipation, represented by a frequency and temperature-dependent electron self-energy, $\Sigma(\omega, T)$ [29]. When interparticle interactions between the system particles are absent (as we assume here) we can *exactly* derive all thermal and charge transport coefficients, in the presence of nonzero Σ.

A crucial but subtle complication arises in thermal transport because of this inelastic dissipation. In the presence of a temperature gradient and for small temperature changes, one might expect contributions from the temperature derivative $\partial\Sigma/\partial T$ to enter into the calculated coefficients. That is, owing to the temperature gradient, the particles, which are doing the thermal conduction, experience a different dissipation at different points across the sample. Because this is rather different from the behavior experienced in the presence of an electric field, it appears problematic. One can anticipate that if such terms were present in the response to a temperature gradient but not to an electric field, they would compromise the Onsager reciprocal relations between electrical and thermal response.

Indeed, we will show in this paper how contributions from $\partial\Sigma/\partial T$ are rather elegantly canceled in both the anomalous thermoelectric response coefficients, as well as the anomalous thermal Hall conductivity. We find this restoration of Onsager reciprocity is a natural consequence of the fluctuation-dissipation theorem [30]. We emphasize the fundamental role of this theorem throughout the paper, noting that within the gravitational-pseudopotential approach [16,24], the thermal Einstein relation presumably provides an analogous supporting framework.

Historically, concepts of fluctuations and stochastic processes, and the fluctuation-dissipation theorem, have played an essential role in establishing not only Onsager's reciprocity relations but also in building the foundations of nonequilibrium thermodynamics [31]. Indeed, the fundamental Kadanoff-Baym transport equations [32] have been shown to be equivalent to a stochastic Langevin equation associated with a thermal bath [33,34]. This body of work has focused more on nonequilibrium quantum field theories in particle physics and cosmology rather than in condensed matter systems, but the wider appeal of a more intuitive bath approach, such as we apply here, should be evident.

The remainder of the paper is organized as follows. In Sec. II, we outline general procedures for obtaining transport coefficients within our heat-bath approach and summarize the resulting central formulas. In Sec. III, we provide a detailed derivation of the anomalous thermal Hall conductivity κ_{xy} which incorporates the fundamental fluctuation-dissipation relation. Numerical implications of our derived transport coefficient formulas are discussed in Sec. IV, emphasizing the interplay of Berry curvature and inelastic scattering. This is presented in the context of the anomalous WF law as well as for an alternative thermoelectric transport ratio. Section V contains our conclusions and outlook. In addition, we make a number of details available in several appendices.

II. GENERAL DISCUSSION AND SUMMARY OF THE FORMULAS

A. General definitions

Thermoelectric transport involves the response of charge (transport) current density $\mathbf{J}^e_{\rm tr}$ and heat (transport) current density $\mathbf{J}^h_{\rm tr}$ in the presence of an electric field $\mathbf{E}$ and temperature gradient $\mathbf{\Theta} \equiv -\nabla T$. We define four tensorial transport coefficients as

$$\begin{bmatrix}\mathbf{J}^e_{\rm tr}\\ \mathbf{J}^h_{\rm tr}\end{bmatrix} \equiv \begin{bmatrix}\overleftrightarrow{\sigma} & \overleftrightarrow{\beta}\\ \overleftrightarrow{\gamma} & \overleftrightarrow{\kappa}\end{bmatrix}\begin{bmatrix}\mathbf{E}\\ \mathbf{\Theta}\end{bmatrix} = \begin{bmatrix}\overleftrightarrow{\mathcal{L}}^{00} & \overleftrightarrow{\mathcal{L}}^{01}\\ \overleftrightarrow{\mathcal{L}}^{10} & \overleftrightarrow{\mathcal{L}}^{11}\end{bmatrix}\begin{bmatrix}\mathbf{E}\\ \mathbf{\Theta}\end{bmatrix} \tag{2.1a}$$

$$= \begin{bmatrix}\overleftrightarrow{L}^{e,e} & \overleftrightarrow{L}^{e,h} - \frac{\partial \mathbf{M}^e}{\partial T}\times\\ \overleftrightarrow{L}^{h,e} - \mathbf{M}^e\times & \overleftrightarrow{L}^{h,h} - \frac{\partial \mathbf{M}^h}{\partial T}\times\end{bmatrix}\begin{bmatrix}\mathbf{E}\\ \mathbf{\Theta}\end{bmatrix}. \tag{2.1b}$$

Here, $\overleftrightarrow{\sigma}$ and $\overleftrightarrow{\kappa}$ are the electrical and thermal conductivities, respectively, and $\overleftrightarrow{\gamma}$ and $\overleftrightarrow{\beta}$ represent the cross-thermoelectric terms which are related to one another by the Onsager reciprocal relation. In this paper, we ignore the fact that in experiments $\overleftrightarrow{\kappa}$ is different from the measured thermal conductivity due to an open-circuit condition, which our calculations indicate will cause only a small correction to the anomalous WF ratio in the clean limit [35]. For later convenience, we also introduce a more compact notation, $\overleftrightarrow{\mathcal{L}}^{\alpha\beta}$ with $\{\alpha, \beta\} = \{0, 1\}$, for these coefficients.

To calculate $\mathbf{J}^e_{\rm tr}$ and $\mathbf{J}^h_{\rm tr}$, one first computes the so-called "microscopic" current densities in the presence of external perturbations $\mathbf{E}$ and $\boldsymbol{\Theta}$, giving rise to the $\overleftrightarrow{L}^{ij}$ contribution in Eq. (2.1b), with $\{i, j\} = \{e, h\}$. It is well-known that these "microscopic" currents are different from the transport currents [2,24] and that, to obtain the latter, physically measurable currents one needs to subtract the divergence-free currents due to the charge magnetization $\mathbf{M}^e$ and the heat magnetization $\mathbf{M}^h$. From Eq. (2.1b), this subtraction is seen to affect only the transverse transport coefficients.

B. Central results

In this paper, we will show how both the coefficients $\overleftrightarrow{L}^{i,j}$ and the magnetization derivative $\partial \mathbf{M}^j/\partial T$ in Eq. (2.1b) can be expressed in terms of the single-particle Green's function. The Green's functions as specified include both retarded ($G_{\rm R}$) and advanced ($G_{\rm A}$) forms which, importantly, depend on their respective self-energies, $\Sigma_{\rm R}$ and $\Sigma_{\rm A}$. We set $\hbar = k_B = a = 1$ in the following, where a is the lattice spacing. Throughout, the summation over repeated indices is assumed.

The central result of the formalism in this paper is a consolidated form for *all* anomalous transport coefficients derived in the presence of inelastic dissipative processes. This is given by

$$\mathcal{L}^{\alpha\beta}_{ij} = \epsilon_{zij}\epsilon_{zab}\frac{q^{2-\alpha-\beta}}{2T^\beta}\int \frac{d\mathbf{k}}{(2\pi)^2}\left\{\int \frac{d\omega}{2\pi}\mathrm{Tr}[v_a G_{\rm R} v_b G_{\rm A}]\omega^{\alpha+\beta} n_F^{(1)} + \oint \frac{d\omega}{2\pi}\mathrm{Tr}[v_b(\partial_\omega G)v_a G] I^{\alpha\beta}(\omega)\right\}, \tag{2.2}$$

which applies to a general multiorbital lattice model in two dimensions. For brevity and when it is self-evident, we have suppressed arguments of the right-hand side variables; we note that ϵ refers to the fully antisymmetric tensor with $\{i, j\} = \{x, y\}$. $q = -e < 0$ is the charge of electrons. The trace $\mathrm{Tr}[\cdots]$ is with respect to the multiorbital subspace. $v_a \equiv \partial_{k_a} H(\mathbf{k})$ is the velocity, where $H(\mathbf{k})$ is the corresponding multiorbital Hamiltonian. In the first term inside the curly bracket of Eq. (2.2), $n_F^{(1)} \equiv -\partial_\omega n_F(\omega)$ where $n_F(\omega)$ is the Fermi-Dirac distribution function. In the second term, the $\oint d\omega$ integral is along the Schwinger-Keldysh contour in Fig. 2. The G in $\mathrm{Tr}[v_b(\partial_\omega G)v_a G]$ can be either $G_{\rm R}$ or $G_{\rm A}$, depending on whether ω is on the forward or backward branch of the contour. The functions $I^{\alpha\beta}(\omega)$ are given by

$$I^{00}(\omega) = n_F(\omega), \tag{2.3a}$$

$$I^{01}(\omega) = I^{10}(\omega) = \omega n_F(\omega) + \frac{1}{\beta}\ln(1 + e^{-\beta\omega}), \tag{2.3b}$$

$$I^{11}(\omega) = \frac{1}{\beta^2}\int_{\beta\omega}^{\infty} \frac{x^2}{4\cosh^2(x/2)}dx, \tag{2.3c}$$

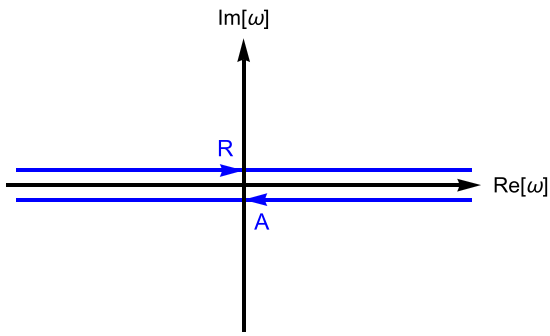

FIG. 2. The contour for $\oint d\omega$ in Eq. (2.2). R and A indicate that the Green's functions corresponding to the two branches are retarded and advanced, respectively.

where $\beta = 1/T$.

When $\Sigma_{\rm R} = \Sigma_{\rm A} \equiv 0$, the four transport coefficients $\mathcal{L}^{\alpha\beta}_{ij}$ reduce to known results in the literature. They can be put into the following compact form [36]:

$$\mathcal{L}^{\alpha\beta}_{xy} = \frac{q^{2-\alpha-\beta}}{T^\beta}\int d\omega\, \widetilde{\sigma}_{xy}(\omega)\omega^{\alpha+\beta} n_F^{(1)}(\omega), \tag{2.4}$$

where

$$\widetilde{\sigma}_{xy}(\omega) \equiv \sum_n \int \frac{d\mathbf{k}}{(2\pi)^2}\Omega^z_n(\mathbf{k})\Theta(\omega - \xi_n(\mathbf{k})). \tag{2.5}$$

Here, $\Omega^z_n(\mathbf{k})$ is the Berry curvature of the nth energy band of $H(\mathbf{k})$, with $\xi_n(\mathbf{k})$ the corresponding energy eigenvalue, and $\Theta(x)$ is the Heaviside function. At $T = 0$, one can replace $\widetilde{\sigma}_{xy}(\omega)$ with $\widetilde{\sigma}_{xy}(\omega = 0)$ in the integrand of Eq. (2.4) and readily verify that (1) σ_{xy} and κ_{xy} satisfy the WF relation

$$\frac{\kappa_{xy}}{T\sigma_{xy}} = L_0 \equiv \frac{\pi^2}{3}\left(\frac{k_B}{q}\right)^2, \tag{2.6}$$

and (2) β_{xy} and σ_{xy} satisfy the Mott relation

$$\beta_{xy} = \frac{\pi^2}{3}\frac{k_B}{q}k_B T\frac{\partial\widetilde{\sigma}_{xy}(\omega)}{\partial\omega}\bigg|_{\omega=0}. \tag{2.7}$$

Here we have restored k_B. These results will not apply except at the lowest temperatures where inelastic dissipation is negligible.

III. DERIVATION OF ANOMALOUS THERMAL TRANSPORT COEFFICIENTS

A. Introduction to the heat-bath approach

We focus in this section on the thermal Hall coefficient κ_{xy} as given in Eq. (2.2). This derivation presents a prototype for the other transport coefficients [36].

Figure 1 presents a schematic illustration of our system. It consists of two parts, the primary component involves electrons associated with multiple orbitals and confined to a lattice. The secondary system is a heat bath with an infinite number of localized electronic degrees of freedom. The corresponding Hamiltonian consists of three components referring to the particles (s), the bath (b), and their coupling (sb) such that $H = H_s + H_b + H_{sb}$ with

$$H_s = \sum_{ij}\sum_{mn} \psi^\dagger_{im} H_{im,jn}\psi_{jn} - \mu_F \sum_{im} \psi^\dagger_{im}\psi_{im}, \quad (3.1a)$$

$$H_b = \sum_{i\alpha} a_\alpha \phi^\dagger_{i\alpha}\phi_{i\alpha}, \quad (3.1b)$$

$$H_{sb} = \sum_{i\alpha m} \eta_\alpha \psi^\dagger_{im}\phi_{i\alpha} + \text{H.c.} \quad (3.1c)$$

H_s describes a general tight-binding model on a lattice where $\{i, j\}$ represents lattice sites and $\{m, n\}$ reflects orbital degrees of freedom. Here ψ_{im} represents the annihilation operators of the particles of orbital m and at site i in the system, and $H_{im,jn}$ is the corresponding tunneling between i and j. Finally, μ_F is the chemical potential.

In the heat-bath component described by Hamiltonian H_b, $\phi_{i\alpha}$ is the corresponding annihilation operator at site i, while α labels a characteristic quantum number which, for definiteness, is taken to assume a continuous spectrum [37]. We have also assumed that at equilibrium the heat bath is translationally invariant so the energy level a_α is independent of site index i. The coupling constant η_α in H_{sb} is similarly spatially independent reflecting translational invariance.

From the Hamiltonian H, one can write down two coupled equations of motion (EOM) for both ψ_{im} and $\phi_{i\alpha}$ fields. Because of the local nature of the heat-bath particles, one can integrate out the heat bath and obtain

$$i\frac{\partial}{\partial t}\psi_{im}(t) = \sum_{jn}(H_{im,jn} - \mu_F\delta_{ij}\delta_{mn})\psi_{jn}(t) + D_i(t) + \int_{-t_0}^{t} dt'\,\Sigma(t-t')\psi_{im}(t'), \quad (3.2)$$

where

$$D_i(t) = \sum_\alpha \eta_\alpha \exp\big(-ia_\alpha(t-t_0)\big)\phi_{i\alpha}(t_0), \quad (3.3a)$$

$$\Sigma(t) = \sum_\alpha |\eta_\alpha|^2(-i)e^{-ia_\alpha t}. \quad (3.3b)$$

Here, the initial time t_0 can be set to $-\infty$ at the end of the procedure. Equation (3.2) takes the form associated with generalized Langevin dynamics [34,38]; this equation shows that ψ_{im} evolves with time under the influence of the tight-binding Hamiltonian H_s, but is also subject to the random force $D_i(t)$ with an embedding self-energy kernel $\Sigma(t-t')$ representing a retarded effect of the frictional force [38].

A local thermal equilibrium of the ψ_{im} field is maintained through a thermal ensemble average of the heat bath field $\phi_{i\alpha}$ or, equivalently, the source field D_i. We assume that $\phi_{i\alpha}$ satisfies ideal Fermi-Dirac statistics and define $\langle\cdots\rangle$ to represent a thermal ensemble average, so $\langle\phi^\dagger_{i\alpha}(t_0)\phi_{j\beta}(t_0)\rangle = \delta_{ij}\delta_{\alpha\beta}n_F(a_\alpha)$ at time t_0. We then find

$$\langle D^\dagger_i(t)D_j(t')\rangle = \delta_{ij}\sum_\alpha |\eta_\alpha|^2 e^{ia_\alpha(t-t')}n_F(a_\alpha). \quad (3.4)$$

The Fourier transformation of this relation in frequency and $\mathbf{k}$ space leads to [39]

$$\langle D^\dagger D\rangle(\omega) = -2\mathrm{Im}\Sigma(\omega)n_F(\omega), \quad (3.5)$$

which importantly represents a generalized fluctuation-dissipation theorem. The left-hand side characterizes fluctuations of the bath degrees of freedom while the right-hand side depends on the imaginary part of the retarded self-energy Σ_R of the particles in the system and thus corresponds to the dissipation they experience. Equation (3.5) will play an important role in our derivation of transport coefficients in Sec. III B.

Here $\Sigma_\mathrm{R} \equiv \mathrm{Re}\Sigma + i\mathrm{Im}\Sigma$ is the Fourier transform of $\Theta(t)\Sigma(t)$. From Eq. (3.3b), we have

$$\mathrm{Im}\Sigma(\omega) \equiv -\pi\sum_\alpha |\eta_\alpha|^2\delta(\omega - a_\alpha), \quad (3.6a)$$

$$\mathrm{Re}\Sigma(\omega) \equiv \mathcal{P}\int \frac{d\omega'}{\pi}\frac{\mathrm{Im}\Sigma(\omega')}{\omega'-\omega}, \quad (3.6b)$$

where $\mathcal{P}$ represents the Cauchy principal value.

From the Fourier transform of Eq. (3.2), one can derive

$$G^<_{m,n}(\mathbf{k},\omega) \equiv i\langle\psi^\dagger_m(\mathbf{k},\omega)\psi_n(\mathbf{k},\omega)\rangle = i[G_\mathrm{R}(\mathbf{k},\omega)\langle D^\dagger D\rangle(\omega)G_A(\mathbf{k},\omega)]_{m,n}, \quad (3.7)$$

where $G^<$ is the conventional lesser Green's function [40]. Just like G_R and G_A, $G^<$ is a matrix in the orbital subspace. Because the heat-bath degrees of freedom are orbitally independent, both $\langle D^\dagger D\rangle(\omega)$ and $\Sigma(\omega)$ are local functions proportional to the identity matrix in this space.

In the presence of external perturbations, $\mathbf{E}$ or $\boldsymbol{\Theta} = -\nabla T$, $G^<$ deviates from its equilibrium value in Eq. (3.7), and the deviation can be computed to linear order in $\mathbf{E}$ or $\boldsymbol{\Theta}$ using standard perturbation theory. From the perturbed $G^<$ one can then compute the "microscopic" charge and heat-current densities, $\langle\hat{\mathbf{J}}^e\rangle_{\mathbf{E},\boldsymbol{\Theta}}$ and $\langle\hat{\mathbf{J}}^h\rangle_{\mathbf{E},\boldsymbol{\Theta}}$, from which the transport coefficients can be derived after appropriate magnetization current subtractions.

B. Evaluation of κ_{xy}

As a prototypical example of the subsequent implications for transport, we evaluate the thermal Hall conductivity, which describes a transport heat-current response to the perturbation $\boldsymbol{\Theta}$. The heat-current density operator satisfies the continuity equation [36]. Its expectation value can be written in coordinate and Fourier transform space as

$$\langle\hat{\mathbf{J}}^h\rangle_{\boldsymbol{\Theta}} = \left\langle\frac{1}{V}\int d\mathbf{x}dt\int d\mathbf{x}'dt'\mathrm{Tr}\left[\psi^\dagger(\mathbf{x}'t')\mathbf{v}(\mathbf{x}',\mathbf{x})\frac{i\overrightarrow{\partial_t} - i\overleftarrow{\partial_{t'}}}{2}\psi(\mathbf{x}t)\right]\right\rangle = \frac{1}{i}\int\frac{d\mathbf{k}}{(2\pi)^2}\frac{d\omega}{2\pi}\mathrm{Tr}[\mathbf{v}(\mathbf{k})\omega G^<_{\boldsymbol{\Theta}}(\mathbf{k},\omega)], \quad (3.8)$$

where, for simplicity, we have switched from a discrete lattice sum $\sum_i$ to a continuous $\int d\mathbf{x}$ integral notation [36], and dropped the orbital index of all operators. V is the spatial volume; $\mathbf{v}$ is the velocity operator defined from H_s. The subscript $\boldsymbol{\Theta}$ in $G^<_{\boldsymbol{\Theta}}$ indicates that this is the perturbed Green's function, whose derivation closely follows that of Eq. (3.7).

In the presence of $\boldsymbol{\Theta}$, the only difference is that in the equation of motion in Eq. (3.2), we now have $D_i \to D_i - \frac{\partial D_i}{\partial T}\mathbf{x}\cdot\boldsymbol{\Theta}$ and $\Sigma \to \Sigma - \frac{\partial \Sigma}{\partial T}\mathbf{x}\cdot\boldsymbol{\Theta}$ to linear order in $\boldsymbol{\Theta}$ [41]. Making these substitutions in Eq. (3.7) leads to

$$G^< \to G^<_{\boldsymbol{\Theta}} = G^< - i\left[G_{\mathrm{R}}\frac{\partial\Sigma_{\mathrm{R}}}{\partial T}\mathbf{x}G_{\mathrm{R}}\langle D^\dagger D\rangle G_{\mathrm{A}} + G_{\mathrm{R}}\langle D^\dagger D\rangle G_{\mathrm{A}}\frac{\partial\Sigma_{\mathrm{A}}}{\partial T}\mathbf{x}G_{\mathrm{A}} + G_{\mathrm{R}}\left(\left\langle\frac{\partial D^\dagger}{\partial T}D\right\rangle + \left\langle D^\dagger\frac{\partial D}{\partial T}\right\rangle\right)\mathbf{x}G_{\mathrm{A}}\right]\cdot\boldsymbol{\Theta}, \tag{3.9}$$

where we have suppressed the arguments $\mathbf{k}$ and ω of all functions [42]. Substituting the result for $G^<_{\boldsymbol{\Theta}}$ into Eq. (3.8) and replacing $\mathbf{x}$ with $i\boldsymbol{\nabla}_{\mathbf{k}}$ [43] leads to $\langle J^h_i\rangle_{\boldsymbol{\Theta}} = L^{h,h}_{ij}\Theta_j$ with

$$L^{h,h}_{ij} = -\frac{\epsilon_{zij}\epsilon_{zab}}{2}\int\frac{d\mathbf{k}}{(2\pi)^2}\int\frac{d\omega}{2\pi}\mathrm{Tr}\left\{v_a\omega\left[G_{\mathrm{R}}\frac{\partial\Sigma_{\mathrm{R}}}{\partial T}\partial_b G^< + G^<\frac{\partial\Sigma_{\mathrm{A}}}{\partial T}\partial_b G_{\mathrm{A}} + iG_{\mathrm{R}}\left(\frac{\partial}{\partial T}\langle D^\dagger D\rangle\right)\partial_b G_{\mathrm{A}}\right]\right\}, \tag{3.10}$$

where $\partial_b \equiv \partial_{k_b}$. The $\epsilon_{zij}\epsilon_{zab}/2$ factor is included since only the $i \leftrightarrow j$ antisymmetric part contributes to anomalous thermal Hall transport.

As discussed in Sec. II, $\langle\hat{\mathbf{J}}^h\rangle_{\boldsymbol{\Theta}}$ is not the transport current. To obtain the latter, one needs to subtract the heat magnetization current, $\partial\mathbf{M}^h/\partial T\times\boldsymbol{\Theta}$, from $\langle\hat{\mathbf{J}}^h\rangle_{\boldsymbol{\Theta}}$. An expression for $\mathbf{M}^h$ can be derived [36] by considering a semi-infinite system with an edge and assuming that the chemical potential μ_F varies slowly from its bulk value far away from the edge to $\mu_F = -\infty$ (i.e., its corresponding vacuum value) just right outside of the edge. Because of spontaneous time-reversal-symmetry breaking due to orbital motion, there is a heat current (as well as an electric current) flowing along the edge, whose density $\mathbf{J}^h_{\mathrm{edge}}$ can be related to the bulk heat magnetization by $\mathbf{J}^h_{\mathrm{edge}} = \boldsymbol{\nabla}\mu_F\times\frac{\partial\mathbf{M}^h}{\partial\mu_F}$, where $\boldsymbol{\nabla}\mu_F$ is the spatial gradient of μ_F due to the edge. $\mathbf{J}^h_{\mathrm{edge}}$ can be evaluated just as $\langle\mathbf{J}^h\rangle_{\boldsymbol{\Theta}}$ by including $(1-\partial\Sigma/\partial\mu_F)\mathbf{x}\cdot\boldsymbol{\nabla}\mu_F$ as a perturbation to the EOM in (the time-frequency Fourier transformed) Eq. (3.2). From $\mathbf{J}^h_{\mathrm{edge}}$, one then obtains $\partial\mathbf{M}^h/\partial\mu_F$, and integrating over μ_F yields

$$M^h_z = \frac{\epsilon_{zij}}{2}\int\frac{d\mathbf{k}}{(2\pi)^2}\oint\frac{d\omega}{2\pi}\mathrm{Tr}[v_i(\partial_\omega G)v_j G]Q(\omega), \tag{3.11a}$$

$$\text{with}\quad Q(\omega) \equiv \frac{\omega}{\beta}\mathrm{Li}_1(-e^{-\beta\omega}) + \frac{1}{\beta^2}\mathrm{Li}_2(-e^{-\beta\omega}), \tag{3.11b}$$

where $\oint d\omega$ is along the contour in Fig. 2. Because we are considering two dimensions, only the z component of $\mathbf{M}^h$ is relevant. In the equation above, $\mathrm{Li}_n(x)$ is the nth polylogarithm function, which is defined in general for arbitrary complex order s and $|z|<1$ by

$$\mathrm{Li}_s(z) = \sum_{k=1}^{\infty}\frac{z^k}{k^s}. \tag{3.12}$$

For $s=1$, $\mathrm{Li}_1(z) = -\ln(1-z)$.

From Eq. (2.1), we obtain

$$\kappa_{ij} = L^{h,h}_{ij} - \epsilon_{izj}\partial M^h_z/\partial T \equiv \kappa^{(1)}_{ij} + \kappa^{(2)}_{ij}, \tag{3.13}$$

where $\kappa^{(1)}_{ij}$ contains all terms that involve $\partial\Sigma/\partial T$ from both $L^{h,h}_{ij}$ and M^h_z, while $\kappa^{(2)}_{ij}$ contains the remainder.

In the following, we show that $\kappa^{(1)}_{ij} = 0$ because of a cancellation due to the fluctuation-dissipation relation in Eq. (3.5). Collecting all $\partial\Sigma/\partial T$ terms from Eq. (3.13), and using Eqs. (3.10), (3.11), and (3.5), we find

$$\kappa^{(1)}_{ij} = -\frac{\epsilon_{zij}\epsilon_{zab}}{2}\int\frac{d\mathbf{k}}{(2\pi)^2}\int\frac{d\omega}{2\pi}\mathrm{Tr}\left[\omega v_a G_{\mathrm{R}}\frac{\partial\Sigma_{\mathrm{R}}}{\partial T}\partial_b G^< + \omega v_a G^<\frac{\partial\Sigma_{\mathrm{A}}}{\partial T}\partial_b G_{\mathrm{A}} + \omega v_a G_{\mathrm{R}}\frac{\partial(-2i\mathrm{Im}\Sigma)}{\partial T}\partial_b G_{\mathrm{A}} n_F\right]$$
$$+\frac{\epsilon_{zij}\epsilon_{zab}}{2}\int\frac{d\mathbf{k}}{(2\pi)^2}\oint\frac{d\omega}{2\pi}\mathrm{Tr}[v_a(\partial_T\partial_\omega G)v_b G]Q \tag{3.14a}$$
$$= \frac{\epsilon_{zij}\epsilon_{zab}}{2}\int\frac{d\mathbf{k}}{(2\pi)^2}\oint\frac{d\omega}{2\pi}\{\mathrm{Tr}[v_a(\partial_T G)v_b G]\omega n_F + (\partial_\omega\mathrm{Tr}[v_a(\partial_T G)v_b G])Q\} \tag{3.14b}$$
$$= 0. \tag{3.14c}$$

The first line comes from $L^{h,h}_{ij}$, while the second arises from $-\epsilon_{izj}\partial M^h_z/\partial T$. In the derivation we have used $G^< = (G_{\mathrm{A}} - G_{\mathrm{R}})n_F$. To arrive at the last line, we have performed an integration by parts over ω in the second term in Eq. (3.14b) and used the identity $\partial_\omega Q = \omega n_F$. *We emphasize that the fluctuation-dissipation relation, Eq. (3.5), is central for the complete cancellation of the $\partial\Sigma/\partial T$ contributions to $\kappa^{(1)}_{ij}$.* This is schematically shown in Fig. 3. A similar cancellation occurs in the derivation of the coefficient β_{xy} [36].

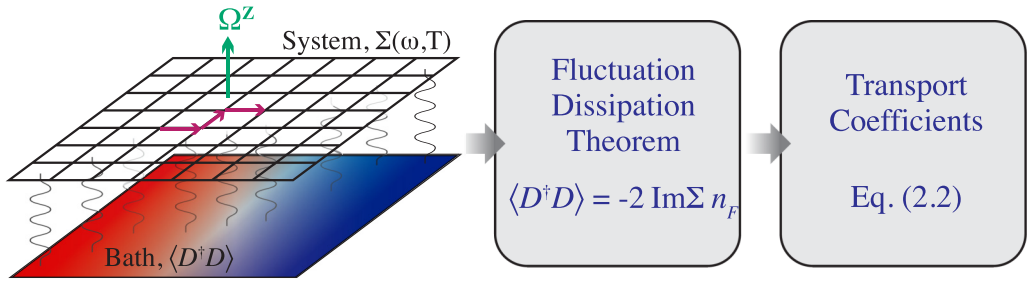

FIG. 3. Schematic figure emphasizing that because the system and heat bath are coupled and in local equilibrium with each other, the electron self-energy Σ originating from the coupling and the heat-bath correlator $\langle D^\dagger D\rangle$ are not independent. Instead, they satisfy the fundamental fluctuation-dissipation relation, expressed in Eq. (3.5), which underpins the notion of local equilibrium. This leads to the simple and rather elegant form of all our derived transport coefficients seen in Eq. (2.2).

What remains in Eq. (3.13) is then

$$\kappa_{ij}^{(2)} = \frac{\epsilon_{zij}\epsilon_{zab}}{2}\int\frac{d\mathbf{k}}{(2\pi)^2}\int\frac{d\omega}{2\pi}\left\{\mathrm{Tr}[\omega v_a G_{\mathrm{R}}(2i\,\mathrm{Im}\Sigma)G_{\mathrm{A}}v_b G_{\mathrm{A}}]\;\partial_T n_F + \oint\frac{d\omega}{2\pi}\mathrm{Tr}[v_a(\partial_\omega G)v_b G]\;\partial_T Q\right\}. \tag{3.15}$$

The first term arises from $L_{ij}^{h,h}$ while the second from $-\epsilon_{izj}\partial M_z^h/\partial T$. Using $G_{\mathrm{R}}^{-1} - G_{\mathrm{A}}^{-1} = -i2\mathrm{Im}\Sigma$, we find that $\kappa_{ij}^{(2)}$ yields the full κ_{xy} of Sec. II B, where we make use of $\partial_T n_F = (\omega/T)n_F^{(1)}$ and $\partial_T Q = -I^{11}(\omega)/T$. This completes our derivation of κ_{xy}.

IV. NUMERICAL IMPLICATIONS

We now explore the numerical implications of our transport coefficient formula, Eq. (2.2). There have been experimental studies of all anomalous coefficients [10–12], with recent emphasis on two important ratios: the first involves a thermoelectric coefficient β_{xy}/σ_{xy} and the second corresponds to the widely studied WF ratio $\kappa_{xy}/(\sigma_{xy}T)$. Importantly, these experiments address the two ratios over the entire temperature range up to and beyond room temperature, where inelastic scattering effects, as in electron-phonon scattering, are expected to play an important role.

While little is known theoretically about how inelastic scattering affects the behavior of the anomalous transport coefficients and their ratios, these effects are necessarily important once the system has departed from the ground state. It is widely believed [11,14] that inelastic scattering leads to a depression rather than an enhancement in the WF ratio once temperature is increased from zero. This assertion is correct only for the longitudinal WF ratio [36]; here we show the situation is different for the anomalous transverse case where Berry-curvature physics becomes important and nonuniversal behavior obtains.

Using Eq. (2.2), we explore the transport properties for two different band structures showing how $\kappa_{xy}/(\sigma_{xy}T)$ can exhibit complex behavior as a result of the distribution of Berry curvatures. We also address the universal behavior of another important ratio β_{xy}/σ_{xy}.

We consider a generic two-band tight-binding model Hamiltonian which supports nonzero Berry curvature effects and is of the general form in $\mathbf{k}$ space,

$$H(\mathbf{k}) = h_0(\mathbf{k}) + \mathbf{h}(\mathbf{k})\cdot\boldsymbol{\sigma} - \mu_{\mathrm{F}}, \tag{4.1}$$

where $\boldsymbol{\sigma} = (\sigma_x, \sigma_y, \sigma_z)$ are the three Pauli matrices defined in 2×2 orbital space. In the following, we assume only one spin component of electrons is populated with a fully polarized magnetic metal in mind. However, we expect that our analysis is applicable to a large class of systems, including, for example, noncollinear antiferromagnets which have received significant attention [12]. Here we address two related variants of this Hamiltonian [36]. One is topological (H_{II}) while the other (H_{I}) is not. The topological case derives from a model of a Chern insulator [44] with complex hopping integrals associated with a staggered magnetic flux through each square lattice plaquette. H_{I} describes a system of two quasi-1D d orbitals also on a square lattice with a spin-orbit coupling that gives rise to nonzero Berry curvature. For simplicity, we defer the detailed parametrizations of both H_{II} and H_{I} to the Appendix [36].

The inelastic contributions to $\Sigma(\omega, T)$ are assumed to arise from electron-phonon coupling [45], which should become relevant at any nonzero temperature. Its effect on longitudinal transport is relatively well understood [36,46] and so serves as a useful baseline.

Quite generally, one models the electron-phonon scattering to be associated with an electron self-energy [40],

$$\mathrm{Im}\Sigma(\omega) = -\pi\int_0^{\omega_D} d\omega'\alpha^2F(\omega')[2n_B(\omega') + n_F(\omega'+\omega) + n_F(\omega'-\omega)], \tag{4.2}$$

where $n_B(\omega) = 1/(e^{\omega/T}-1)$. Here, $\alpha^2F(\omega)$ reflects the coupling [40] and ω_D is the Debye frequency beyond which $\alpha^2F(\omega)$ vanishes. For acoustic phonons, which are dominant, the related spectral function can be modeled by [47]

$$\alpha^2F(\omega) = \lambda(\omega/\omega_D)^2\Theta(\omega_D - |\omega|). \tag{4.3}$$

$\mathrm{Re}\Sigma$ is then obtained by using the Kramers-Kronig relation, Eq. (3.6b).

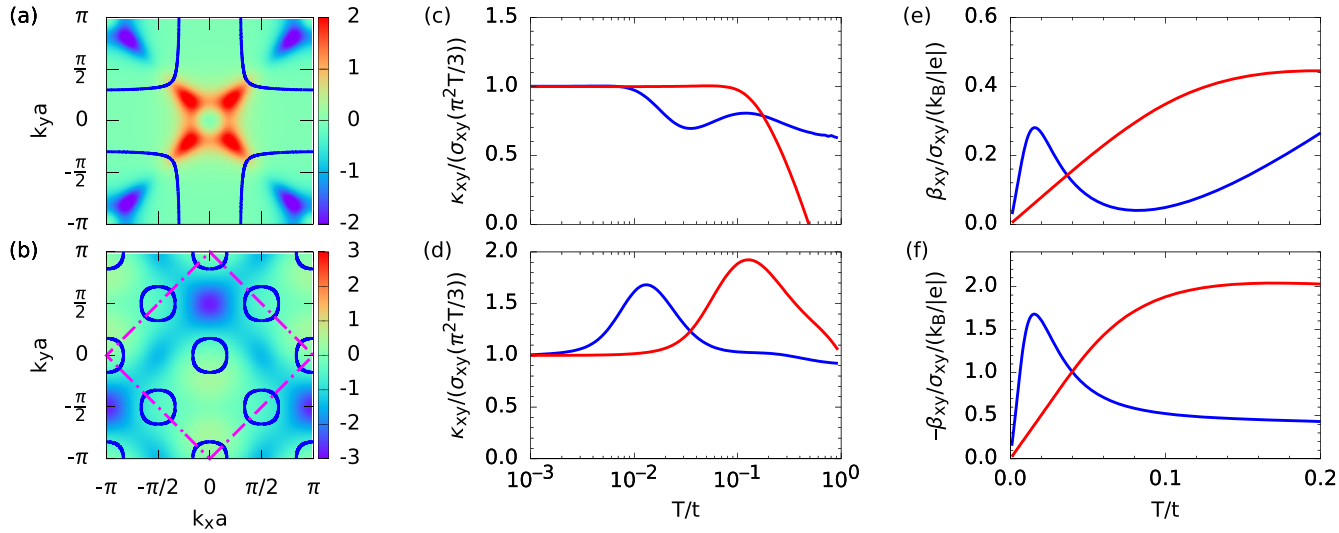

FIG. 4. The effects of two different Berry-curvature distributions, (a) and (b), on anomalous transport coefficient ratios, (c)–(f), showing the effects with (blue) and without (red) dissipation. The Berry curvature is plotted for the lower energy band together with the corresponding Fermi surface contour (blue solid line). The magenta dashed line in (b) denotes the reduced Brillouin zone. Upper panels (a), (c), and (e) are for model H_{I} and lower panels (b), (d), and (f) are for model H_{II}, whose energy bands are topologically nontrivial. Note the additional minus sign in the vertical axis label in (f). For the simulations in (c)–(f), we have chosen the Debye frequency $\omega_D = 0.1t$, where t is the nearest-neighbor hopping integral in each model and the electron-acoustic-phonon coupling strength $\lambda = 5$. A large λ is chosen for a better visualization of inelastic scattering effects.

Figure 4 addresses the behavior of the anomalous WF ratio $\kappa_{xy}/(\sigma_{xy}T)$ for both models. The Berry-curvature distribution for the two models is plotted in Figs. 4(a) and 4(b). Figures 4(c) and 4(d) present plots comparing the behavior with inelastic scattering included (blue) and without (red).

If for the moment we omit inelastic effects, there are some interesting observations to be made. It has been claimed in the literature [12] that, when T increases, σ_{xy} and κ_{xy} sample the same Berry-curvature distribution, but with different weights for a given energy due to the $\omega^{\alpha+\beta}$ factor in Eq. (2.4). This difference in weighting, combined with the dispersion of Berry-curvature distribution with energy, leads to different temperature dependencies of σ_{xy} and κ_{xy}/T and, therefore, to a violation of the WF law once temperature becomes sufficiently high. The direction of the violation of the WF ratio has been argued [12] to be consistent: one always sees a downward deviation of $\kappa_{xy}/(\sigma_{xy}T)$ from the Lorenz number at finite temperature [12].

As can be seen from the red curves in the plots, what we observe (even without dissipation) is rather different. We find the WF ratio can be either enhanced [red curve in Fig. 4(d)] or suppressed [red curve in Fig. 4(c)] relative to the $T = 0$ value. These differences reflect the fact that Berry curvatures from different regions of reciprocal space carry opposite signs and thus compete. Thus, the overall behavior of the WF ratio reflects both the sign competition of Berry curvatures as well as the different frequency weightings in heat and charge transport. Finally, we emphasize that having a topologically nontrivial band is not a necessary condition for an enhanced WF ratio, as shown in Fig. 4(d), red curve, as we have seen a similar enhancement in some trivial band models as well.

Once inelastic scattering is included, the effects of nonzero $\Sigma(\omega, T)$ add to the complications discussed above. With this temperature-dependent dissipation, the association with Berry curvature deriving from Eq. (2.2) is no longer given by Eq. (2.4). Nevertheless, one can still use the latter equation and the concept of Berry curvature as a guideline and infer that the presence of $\Sigma(\omega, T)$ will change the Berry-curvature contributions to each transport coefficient and lead to either an additional upturn deviation or a downturn deviation from the baseline WF ratio. This will be apparent only within the inelastic regime ($T \lesssim \omega_D$).

These violations due to the interplay between the Berry-curvature distribution and inelastic scattering are seen in the two models and plotted as the blue curves in Figs. 4(c) and 4(d). For completeness, we note that finite-temperature enhancements of the WF ratio have been recently observed in a kagome Chern magnet [14]. Overall, our findings highlight the intrinsic challenge of disentangling inelastic scattering from Berry-curvature effects in analyzing experimental data. Moreover, they point out that unlike the longitudinal case, the behavior of the temperature-dependent transverse WF ratio is expected to be highly nonuniversal.

Although we have focused our discussion on the ratio $\kappa_{xy}/(\sigma_{xy}T)$, we point out that this sign competition (and entanglement of inelastic dissipation with Berry curvature) is reflected in all anomalous transport, not just in the ratios but also in σ_{xy} and κ_{xy}/T, as shown by the red and blue curves in Figs. 5(b) and 5(d). We also emphasize that there is a similar interplay between Berry curvature and inelastic self-energy effects in the anomalous thermoelectric parameter, β_{xy}, as shown in Fig. 5(c). However, interestingly, we find that, in contrast to $\kappa_{xy}/(\sigma_{xy}T)$, the ratio β_{xy}/σ_{xy} seems to exhibit a universal behavior: We consistently find that the low-temperature slope of $|\beta_{xy}/\sigma_{xy}|$ appears to be enhanced by inelastic scattering. This is shown for the model H_{I} in Fig. 4(e), while Fig. 4(f) plots the corresponding result for the topological case of H_{II}. For the latter, the same enhancement appears despite the fact

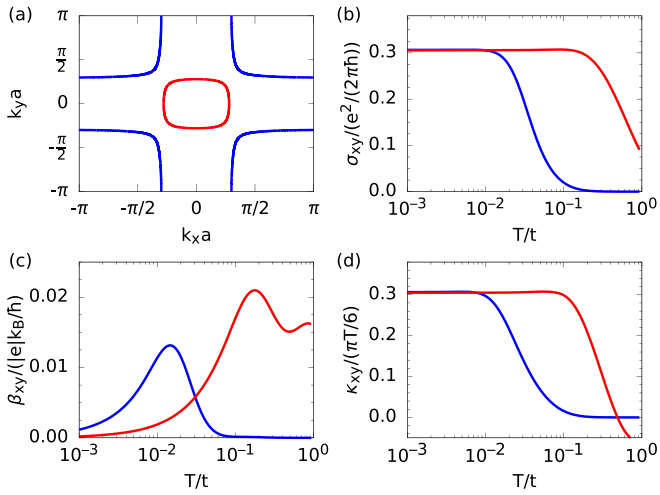

FIG. 5. Fermi surface (a) and complete set of anomalous transport coefficients (b)–(d) for the nontopological model, $H_{\rm I}$. Similar results for $H_{\rm II}$ are presented in the Appendix. In (b)–(d), blue and red lines correspond to results with and without inelastic scattering effects, respectively. Note that the transport coefficient γ_{xy} is not independent (due to the Onsager relation) and not plotted here.

that β_{xy}/σ_{xy} now has the opposite sign [48]. We can speculate, moreover, that our results may provide an explanation for the recently observed enhancement of $|\beta_{xy}/\sigma_{xy}|$ at $T \lesssim 200$ K in the kagome Chern magnet $TbMn_6Sn_6$ [14], although a much more detailed study is needed to confirm this.

We believe this universal enhancement of the ratio β_{xy}/σ_{xy} can be roughly understood as follows. We first notice that, in the absence of inelastic scattering, the ratio can be interpreted as a ratio between the transverse flow of thermal entropy and that of charge, both under the influence of Berry curvature [11,12,49], averaged over different energy eigenstates. Note that σ_{xy} can be written as a sum of Berry curvature from *all filled* states as incorporated in the occupation number n_F. In contrast, β_{xy} is a sum of the same Berry curvature but now convoluted with the thermal entropy—I^{01} in Eq. (2.3b)—which is nonzero only for *partially occupied states* that lie within an energy shell $\sim T$ near the Fermi level.

Now, if we include the self-energy Σ, σ_{xy} and β_{xy} respond quite differently due to the key difference between the two thermal factors, n_F and I^{01}. At low temperature, Σ is small and its effect is significant only on states within an energy window $\sim|\Sigma|$ near the Fermi level, not those deep in the Fermi sea. Consequently, σ_{xy} is roughly unchanged [see curves at $T/t \lesssim 0.01$ in Fig. 5(b)], while β_{xy} is much more strongly enhanced by the presence of Σ [see Fig. 5(c)]. This latter enhancement comes from an energy broadening due to $\mathrm{Im}\Sigma$, which has a similar effect on thermal entropy as an increase of temperature. In summary, the net effect of Σ at low temperature is an overall enhancement of β_{xy} and of $|\beta_{xy}/\sigma_{xy}|$ as well.

V. CONCLUSIONS AND OUTLOOK

This paper provides a basis for understanding what happens to anomalous transport properties when temperature is increased beyond the lowest temperature regime. We consider this important question, relevant to a wide class of experiments (as phonons are inevitably present), in the context of anomalous thermal Hall and other anomalous thermoelectric transport coefficients. Our methodology addresses an interesting paradox posed when thinking about how a temperature-dependent self-energy can be consistently addressed in the presence of a thermal gradient. Here we emphasize the advantages of a bath approach as distinct from Luttinger's somewhat controversial scheme [18–23].

Part of the failure to address finite temperature and attendant inelastic scattering in past theoretical literature is likely based on the presumption that these effects in the transverse channel are not that different from those in the longitudinal case. On this basis, one might expect that inelasticity universally suppresses the WF ratio.

We show here this reasoning does not hold and that the effects of inelasticity in the transverse channel are strongly intertwined with the detailed distribution of the Berry curvature. Importantly, there are few universal features one can predict in advance about the temperature-dependent behavior of the transverse WF ratio. By contrast, we are able to identify a transport ratio involving a thermoelectric response, β_{xy}/σ_{xy}, which exhibits significant universality in the low-temperature regime; importantly, this occurs even in the presence of Berry curvature and inelastic dissipation. While there is some experimental support for both these observations [14], it is hoped that these effects and the expected universality can be explored in more detail in future literature.

Our heat-bath approach leads to a consolidated formula for the entire class of transport coefficients. Indeed, bath approaches have been advocated rather widely within different subfields of the physics community, particularly for electric-field-driven transport. We argue that such approaches are most ideally suited to situations when a temperature gradient or heat current is present, which is not where the prior widespread interest has been. We show here our bath approach provides a more intuitive route to thermal transport and also reveals the fundamental role played by the fluctuation-dissipation theorem.

Also notable is that our heat-bath approach is readily adapted to address transverse thermal transport in a small magnetic field in the presence of inelastic processes; this is associated with conventional thermoelectric and thermal Hall transport. Here, as in the present paper and for a generic multiband lattice model [50], one can derive a consolidated set of transport coefficients.

For concreteness, we have emphasized inelastic dissipation which originates from one particular mechanism, namely, electron-phonon scattering. Nevertheless, we expect our consolidated formulas for all thermal and charge transport coefficients should be applicable to alternative models with different inelastic processes underlying the self energy.

Thus we are led to speculate that, while our calculations are exact in the absence of interparticle interactions, they may also describe interparticle interaction effects provided these are associated with a local self-energy. In this way, we subscribe to the philosophy in the literature surrounding the Kadanoff-Baym approach to nonequilibrium transport which involves interacting particles. Indeed, the Kadanoff-Baym equation has been reinterpreted as a generalized Langevin equation with

noninteracting particles coupled to a heat bath [34], where the bath is assumed to give rise to self-energy contributions deriving from many-body effects.

As we look to the future, it will be interesting to investigate whether our results can be applied to study systems having a local self-energy of the form which appears in studies of quantum criticality. Here one encounters rather violent quantum fluctuation effects which make it problematic to address anomalous thermal transport. Additional directions involve a generalization to three-dimensional topological materials such as Weyl semimetals [51]. More challenging, finally, is to consider the effects of a **k**-dependent self-energy originating from the heat bath. Including these nonlocal effects will be particularly complicated by the fact that the heat bath degrees of freedom can also carry currents if the particles are not localized. A proper treatment of both the system and heat bath on an equal footing is needed to preserve the charge and energy conservation laws. These are crucial for ensuring that (in the language of Kubo-like diagrammatic approaches) vertex-correction contributions to transport coefficients are properly included.

ACKNOWLEDGMENTS

We thank Michael Levin for insightful discussions and Qijin Chen for past collaboration on related subjects. We are grateful to Kamran Behnia and Shuang Jia for their comments on the paper. This work was primarily funded by the University of Chicago Materials Research Science and Engineering Center through the National Science Foundation under Grant No. DMR-1420709. It is completed in part with resources provided by the University of Chicago's Research Computing Center. R.B. was supported by Département de physique, Université de Montréal.

APPENDIX A: COMPARISON OF EQ. (2.2) TO THE LITERATURE

It is important to emphasize that the central results of this paper given in Eq. (2.2) involve the full Green's functions which depend on the self-energy $\Sigma(\omega, T)$. Expressions for the anomalous transport coefficients in the presence of inelastic scattering allow us to address finite temperatures. As far as we are aware, none of these equations have appeared in the literature. However, when we drop $\Sigma(\omega, T)$ our results for the Hall conductivity [52,53], for the Nernst coefficient [3,54], and for the thermal Hall conductivity [2,51,55] can be found elsewhere. What is also important to emphasize is that, without dynamical self-energy effects, there are many equivalent ways of rewriting these Green's function-based equations, using different schemes to do a partial integration over frequency. Notably, however, this equivalence disappears when $\Sigma(\omega, T)$ is introduced since the operation of inserting $\Sigma(\omega, T)$ in Green's functions in general does not commute with an integration by parts over ω. Thus, only certain representations of these equations are correct, in the presence of inelastic dissipation.

We also emphasize that Eq. (2.2) incorporates the proper subtraction of the divergenceless charge and heat magnetization currents. In our work we, thereby, derive expressions for the spontaneous orbital charge and heat magnetizations [26,27,56,57], $\mathbf{M}^e$ and $\mathbf{M}^h$, in the presence of $\Sigma(\omega, T)$, given in the following Eqs. (E5) and (E8). We note that, in the absence of $\Sigma(\omega, T)$, an expression for $\mathbf{M}^e$ in terms of Berry curvature [see Eq. (E9)] is well-established in the literature while that of $\mathbf{M}^h$ is still controversial [2,18,28]. However, establishing the effects of including $\Sigma(\omega, T)$ on both $\mathbf{M}^e$ and $\mathbf{M}^h$ is unique to this paper.

APPENDIX B: MODEL HAMILTONIANS

In Sec. IV of the main text, we have looked at two different two-band Hamiltonians on a square lattice of the form of $H(\mathbf{k})$ in Eq. (4.1). The model we call $H_{\rm I}$ derives from a two-band system which supports an anomalous Hall effect; it is associated with ferromagnetic metals with active $\{d_{xz}, d_{yz}\}$ orbitals [58]. Written in the form as in Eq. (4.1), $H_{\rm I}$ corresponds to

$$h_0(\mathbf{k}) = -t(\cos k_x + \cos k_y), \tag{B1a}$$

$$h_x(\mathbf{k}) = 4t' \sin k_x \sin k_y, \tag{B1b}$$

$$h_y(\mathbf{k}) = -\lambda_{\rm soc}, \tag{B1c}$$

$$h_z(\mathbf{k}) = -t(\cos k_x - \cos k_y). \tag{B1d}$$

Here $\lambda_{\rm soc}$ is the strength of the spin-orbit coupling. t, t' are tight-binding hopping parameters.

The second Hamiltonian we study, called $H_{\rm II}$, is derived from a model that has been used to construct flat bands with nonzero Chern number and to investigate the possibility of a fractional Chern insulator [44]. The same model has also been recently exploited to understand the interplay of quantum geometry and superconducting fluctuations in the superfluid phase stiffness [59,60]. For this model, we take $H_{\rm II}(\mathbf{k}) = h_0(\mathbf{k}) + \mathbf{h}(\mathbf{k}) \cdot \boldsymbol{\sigma} - \mu_{\rm F}$, with

$$h_0(\mathbf{k}) = 0, \tag{B2a}$$

$$h_z(\mathbf{k}) = -2t_2\,[\cos(k_x + k_y) - \cos(k_x - k_y)], \tag{B2b}$$

$$h_x(\mathbf{k}) = -2t[\cos(\phi + k_y)\cos k_y + \cos(\phi - k_y)\cos k_x], \tag{B2c}$$

$$h_y(\mathbf{k}) = 2t[\sin(\phi + k_y)\cos k_y - \sin(\phi - k_y)\cos k_x]. \tag{B2d}$$

Here, t and t_2 denote the magnitudes of the nearest-neighbor and the second-nearest-neighbor hopping integrals and ϕ describes a phase associated with the nearest-neighbor hopping. In the original model, the sign of ϕ depends on the spin. For the spin-$\downarrow$ component, we consider, $\phi = -\pi/4$.

The two energy bands of $H_{\rm II}$ carry opposite Chern numbers, $C_- = -1$ ($C_+ = +1$) for the lower (upper) band. This can be also seen from Fig. 4 which shows that the Berry-curvature distribution of the lower band is dominated by negative contributions. For our calculation, we use the following definitions for the Berry connection $\boldsymbol{\mathcal{A}}_n(\mathbf{k})$, Berry curvature $\boldsymbol{\Omega}_n(\mathbf{k})$, and Chern number C_n [9]:

$$\boldsymbol{\mathcal{A}}_n(\mathbf{k}) = -i\langle u_n|\nabla_{\mathbf{k}}|u_n\rangle, \tag{B3a}$$

$$\boldsymbol{\Omega}_n(\mathbf{k}) = \nabla_{\mathbf{k}} \times \boldsymbol{\mathcal{A}}_n(\mathbf{k}), \tag{B3b}$$

$$C_n = \frac{1}{2\pi}\int d\mathbf{k}\ \Omega_n^z(\mathbf{k}), \tag{B3c}$$

TABLE I. Tight-binding band parameters used for the models considered.

Hamiltonians	Band parameters
$H_{\rm I}$	$(t, t', \lambda_{\rm soc}, \mu_F) = (1, 0.1, 0.25, -1.2)$
$H_{\rm II}$	$(t, t_2, \mu_F) = (1, 1/\sqrt{2}, -2.65)$

where $|u_n\rangle$ is the nth band eigenstate. The $\int d\mathbf{k}$ integral is over the first (reduced) Brillouin zone for $H_{\rm I}$ ($H_{\rm II}$).

In Table I, we list the band parameters used for each model considered in this paper.

APPENDIX C: EFFECTS OF INELASTIC SCATTERING ON THE LONGITUDINAL WF LAW

Although the focus of this paper is on the anomalous transport, for comparison we also give a brief account of the inelastic scattering effects on the longitudinal transport coefficients. Using our heat-bath approach, we can easily derive the expressions for longitudinal transport:

$$\mathcal{L}^{\alpha\beta}_{xx} = \frac{q^{2-\alpha-\beta}}{2T^\beta}\int\frac{d\mathbf{k}}{(2\pi)^2}\int\frac{d\omega}{2\pi}\mathrm{Tr}[v_x\mathcal{A}v_x\mathcal{A}]\omega^{\alpha+\beta}n_F^{(1)}. \quad \text{(C1)}$$

Here again, we have put all longitudinal transport coefficients in a consolidated equation. To be specific, $\{\mathcal{L}^{00}_{xx}, \mathcal{L}^{01}_{xx}, \mathcal{L}^{10}_{xx}, \mathcal{L}^{11}_{xx}\} = \{\sigma_{xx}, \beta_{xx}, \gamma_{xx}, \kappa_{xx}\}$.

Figure 6 presents the corresponding numerical results for a simple square lattice both with and without the inelastic self-energy Σ given in Eq. (4.2). Quite generally, the inclusion of Σ suppresses the magnitude of the longitudinal transport coefficients at low temperatures $T \lesssim \omega_D \ll T_F$, leading to a violation of the WF law [46].

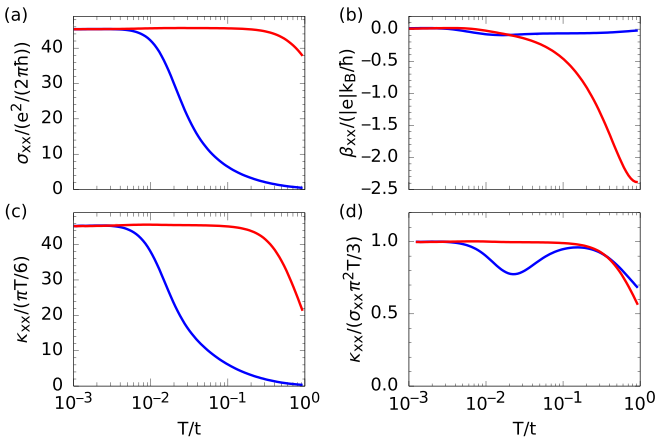

FIG. 6. Longitudinal transport coefficients and WF ratio, both in the presence (blue) and absence (red) of the inelastic self-energy effects. For illustration, we use a simple single-band tight-binding model with the energy dispersion $H(\mathbf{k}) = -2t(\cos k_x + \cos k_y) - \mu_F$ and $\mu_F/t = -1$. For the inelastic self-energy calculation, we have chosen the electron-phonon coupling strength $\lambda = 1$ and the Debye frequency $\omega_D = 0.1t$. A small residual impurity scattering rate $\sim 0.05t$ has been included to regularize σ_{xx} and κ_{xx} so they do not diverge at $T = 0$.

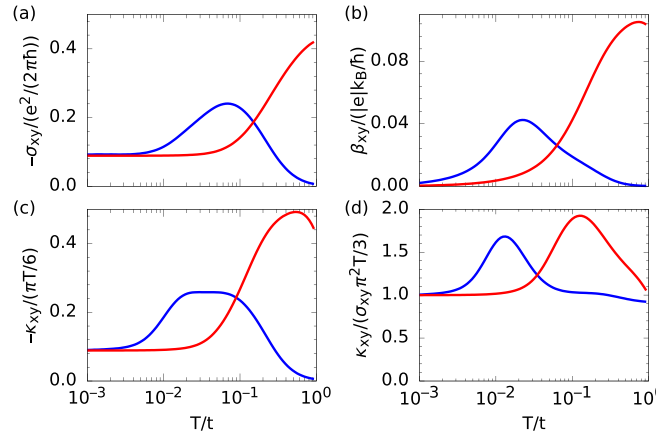

FIG. 7. Numerical results for model $H_{\rm II}$, both with (in blue) and without (in red) the inelastic electron self energy effect. Here we use the parameters $\omega_D = 0.1t$, $\lambda = 5$.

APPENDIX D: NUMERICAL RESULTS OF TRANSPORT COEFFICIENTS FOR THE MODEL $H_{\rm II}$

In Fig. 4 of the main text, we have presented our numerical results for the transport ratios in the case of $H_{\rm II}$, although the individual results for each individual transport coefficient were not shown. They are presented in Fig. 7. The results for σ_{xy}, β_{xy}, and κ_{xy} in the zero-T limit, where the electron-phonon scattering can be neglected, agree with Eq. (2.4). Comparing Fig. 7 to Fig. 6 we see that the temperature dependence of the anomalous transport coefficients can be much more complex than that of their longitudinal counterparts.

APPENDIX E: DERIVATION OF SPONTANEOUS ORBITAL CHARGE AND HEAT MAGNETIZATIONS

In this Appendix, we derive the charge and heat (orbital) magnetizations associated with Berry-curvature effects: $\mathbf{M}^e$ and $\mathbf{M}^h$. These are obtained by relating them to charge and heat boundary currents. To calculate the latter, we imagine the system in the xy plane with a boundary. At local equilibrium, we assume the system's local chemical potential varies slowly from its bulk value μ_F to its vacuum value $\mu_F = -\infty$ at the boundary edge. In addition, the electric potential created by the boundary is also experienced by the bath particles since they carry the same charge as those in the system. Using the local-equilibrium assumption, in response to this potential, the bath particle energy level a_α in Eq. (3.1b) adjusts itself together with μ_F so their difference remains a constant across the whole system; in this way the source field D_i in Eq. (3.2) has an indirect dependence on μ_F.

Within a linear expansion, the above boundary effects can be taken into account by making the following substitution in the EOM in Eq. (3.2):

$$\mu_F \to \mu_F + \nabla\mu_F\cdot\mathbf{x}_i, \quad \text{(E1a)}$$

$$\Sigma \to \Sigma + \frac{\partial\Sigma}{\partial\mu_F}\nabla\mu_F\cdot\mathbf{x}_i, \quad \text{(E1b)}$$

$$D_i \to D_i + \frac{\partial D_i}{\partial\mu_F}\nabla\mu_F\cdot\mathbf{x}_i, \quad \text{(E1c)}$$

where $\nabla\mu_F$ is a constant. We emphasize that it is important to consider simultaneously the μ_F dependence of both Σ and D_i to ensure that the fluctuation-dissipation relation, Eq. (3.5), holds across the whole system, reflecting our assumption of local equilibrium.

The calculation of the boundary charge current density, $\langle \mathbf{J}^e\rangle_{\nabla\mu_F}$, due to the perturbations in Eq. (E1), closely follows that of $\langle \mathbf{J}^h\rangle_{\boldsymbol{\Theta}}$ in Sec. III B of the main text:

$$\begin{aligned}\langle \mathbf{J}^e\rangle_{\nabla\mu_F} &= \frac{q}{i}\int\frac{d\mathbf{k}}{(2\pi)^2}\int\frac{d\omega}{2\pi}\mathrm{Tr}[\mathbf{v}(\mathbf{k})G^<_{\nabla\mu_F}(\mathbf{k},\omega)]\\ &= -iq\int\frac{d\mathbf{k}}{(2\pi)^2}\int\frac{d\omega}{2\pi}\mathrm{Tr}\Big\{\mathbf{v}G_\mathrm{R}\Big(1-\frac{\partial\Sigma_\mathrm{R}}{\partial\mu_F}\Big)\partial_j[G_\mathrm{R}\langle D^\dagger D\rangle G_\mathrm{A}]\\ &\quad+\mathbf{v}G_\mathrm{R}\langle D^\dagger D\rangle G_\mathrm{A}\Big(1-\frac{\partial\Sigma_\mathrm{A}}{\partial\mu_F}\Big)\partial_j G_\mathrm{A}-\mathbf{v}G_\mathrm{R}\Big[\frac{\partial}{\partial\mu_F}\langle D^\dagger D\rangle\Big]\partial_j G_\mathrm{A}\Big\}(\nabla\mu_F)_j\\ &= q\int\frac{d\mathbf{k}}{(2\pi)^2}\oint\frac{d\omega}{2\pi}\mathrm{Tr}\Big[\mathbf{v}G\Big(1-\frac{\partial\Sigma}{\partial\mu_F}\Big)\partial_j G\Big]n_F\ (\nabla\mu_F)_j.\end{aligned}\tag{E2}$$

The subscript $\nabla\mu_F$ in $G^<_{\nabla\mu_F}$ indicates the latter is the perturbed lesser Green's function. When the subscript is not specified, this refers to the bulk. To arrive at the last line in the equation above, we have used the fluctuation-dissipation relation, Eq. (3.5). Here, as before, the integral $\oint$ is along the contour in Fig. 2.

From $\langle \mathbf{J}^e\rangle_{\nabla\mu_F}$, we calculate the charge magnetization by using [24]

$$\langle \mathbf{J}^e\rangle_{\nabla\mu_F} = \nabla\mu_F\times\frac{\partial\mathbf{M}^e}{\partial\mu_F},\tag{E3}$$

which leads to

$$\begin{aligned}\frac{\partial M^e_z}{\partial\mu_F} &= -q\frac{\epsilon_{zij}}{2}\oint\frac{d\omega}{2\pi}\mathrm{Tr}[v_i(\partial_\omega G)v_j G]n_F(\omega)\\ &= -q\frac{\epsilon_{zij}}{2}\oint\frac{d\bar\omega}{2\pi}\mathrm{Tr}[v_i(\partial_{\bar\omega}G)v_j G]n_F(\bar\omega-\mu_F)\\ &= \frac{\partial}{\partial\mu_F}\Big\{q\frac{\epsilon_{zij}}{2}\oint\frac{d\bar\omega}{2\pi}\mathrm{Tr}[v_i(\partial_{\bar\omega}G)v_j G]\times\frac{1}{\beta}\mathrm{Li}_1(-e^{-\beta(\bar\omega-\mu_F)})\Big\}.\end{aligned}\tag{E4}$$

For brevity, we have suppressed $\int\frac{d\mathbf{k}}{(2\pi)^2}$ in these equations. In arriving at the first line, we have used $G(1-\partial_{\mu_F}\Sigma)G = G(1-\partial_\omega\Sigma)G = -\partial_\omega G$ since Σ needs to be a function of $\omega+\mu_F$ (i.e., it cannot depend on the choice of energy reference point). From the first to the second line, we have changed variables $\omega\to\bar\omega=\omega+\mu_F$. The last line is obtained by using $n_F(\omega) = (1/\beta)\partial_\omega\mathrm{Li}_1(-e^{-\beta\omega})$.

Integrating $\partial M^e_z/\partial\mu_F$ over μ_F (from its vacuum to its bulk value) gives

$$M^e_z = q\frac{\epsilon_{zij}}{2}\int\frac{d\mathbf{k}}{(2\pi)^2}\oint\frac{d\omega}{2\pi}\mathrm{Tr}[v_i\partial_\omega G v_j G]\frac{1}{\beta}\mathrm{Li}_1(-e^{-\beta\omega}),\tag{E5}$$

where we have changed the integration variable $\bar\omega$ back to ω and restored $\int\frac{d\mathbf{k}}{(2\pi)^2}$.

The derivation of the heat magnetization follows closely that of M^e_z. The expression for $\partial M^h_z/\partial\mu_F$ differs from that of $\partial M^e_z/\partial\mu_F$ in the first line of Eq. (E4) only by a factor of ω/q, i.e.,

$$\begin{aligned}\frac{\partial M^h_z}{\partial\mu_F} &= -\frac{\epsilon_{zij}}{2}\int\frac{d\mathbf{k}}{(2\pi)^2}\oint\frac{d\omega}{2\pi}\mathrm{Tr}[\omega v_i(\partial_\omega G)v_j G]n_F(\omega)\\ &= \frac{\partial}{\partial\mu_F}\Big\{-\frac{\epsilon_{zij}}{2}\int\frac{d\mathbf{k}}{(2\pi)^2}\oint\frac{d\bar\omega}{2\pi}\mathrm{Tr}[v_i(\partial_{\bar\omega}G)v_j G]Q(\bar\omega-\mu_F)\Big\},\end{aligned}\tag{E6}$$

where Q is defined in Eq. (3.11b) of the main text and reproduced here for convenience:

$$Q(\omega)\equiv\frac{\omega}{\beta}\mathrm{Li}_1(-e^{-\beta\omega})+\frac{1}{\beta^2}\mathrm{Li}_2(-e^{-\beta\omega}).\tag{E7}$$

Integrating $\partial M^h_z/\partial\mu_F$ over μ_F and changing $\bar\omega$ back to ω leads to

$$M^h_z = \frac{\epsilon_{zij}}{2}\int\frac{d\mathbf{k}}{(2\pi)^2}\oint\frac{d\omega}{2\pi}\mathrm{Tr}[v_i(\partial_\omega G)v_j G]Q(\omega).\tag{E8}$$

In the absence of $\Sigma(\omega, T)$, one can compute the ω integrals in Eqs. (E5) and (E8) and obtain

$$\mathbf{M}^e = \sum_n \int \frac{d\mathbf{k}}{(2\pi)^2}\left[q\mathbf{m}_n n_F(\xi_n) - q\mathbf{\Omega}_n \frac{1}{\beta}\mathrm{Li}_1(-e^{-\beta\xi_n})\right], \tag{E9a}$$

$$\mathbf{M}^h = \sum_n \int \frac{d\mathbf{k}}{(2\pi)^2}[\xi_n\mathbf{m}_n n_F(\xi_n) - \mathbf{\Omega}_n Q(\xi_n)], \tag{E9b}$$

where

$$\mathbf{m}_n \equiv \frac{i}{2}\langle\nabla_{\mathbf{k}}u_n|\times[H-\xi_n]|\nabla_{\mathbf{k}}u_n\rangle. \tag{E10}$$

Both $\mathbf{M}^e$ and $\mathbf{M}^h$ contain two parts. The first part involves $q\mathbf{m}_n$ and $\xi_n\mathbf{m}_n$, which can be interpreted as charge and heat orbital magnetic moments of the nth eigenstate, respectively [3,26,28,61]. In a semiclassical picture, these orbital magnetic moments originate from self-rotation of a wave packet [3,61]. The other part of $\mathbf{M}^e$ and $\mathbf{M}^h$ involves the band-dependent Berry curvature, $\mathbf{\Omega}_n(\mathbf{k})$, whose definition is given in Eq. (B3b). This part is associated with the center of mass motion of a wave packet in a semiclassical theory. We note that, in Eq. (E9), we have written the magnetizations in their fully vectorial form to indicate that they also apply to three dimensions as well.

When compared to the literature we find our expression for $\mathbf{M}^e$ in Eq. (E9a) agrees with results in Refs. [3,26,27]. We also find that our expression for the heat magnetization $\mathbf{M}^h$ in Eq. (E9b) coincides with results in Refs. [22,28,61]. However, when comparing with $\mathbf{M}^h$ derived in Ref. [2], we find that Ref. [2] contains an extra term that involves n_F, which arises because of a particular scaling form of the heat-current operator, Eq. (5) of Ref. [2], has been assumed. However, this scaling relation does not hold on a lattice [62]. Therefore, the $\mathbf{M}^h$ result in Ref. [2] cannot be directly applied to a lattice model such as ours.

APPENDIX F: DERIVATIONS OF ANOMALOUS σ_{xy}, γ_{xy} AND β_{xy}

In the main text, we have derived κ_{xy} using our heat-bath approach. In this section, we provide detailed derivations of the other three anomalous transport coefficients, $\{\sigma_{xy}, \gamma_{xy}, \beta_{xy}\}$.

1. Derivation of σ_{xy}

We start with the response to the electric field $\mathbf{E}$. The perturbation due to $\mathbf{E}$ can be written (in $\mathbf{k}$ space) as

$$H'_{\mathbf{E}}(\mathbf{k}) = q\mathbf{v}(\mathbf{k})\cdot\mathbf{E}t, \tag{F1}$$

where we have adopted the temporal gauge $\mathbf{A}_{\mathbf{E}} = -\mathbf{E}t$, where t is the time [63]. It should be understood that $H'_{\mathbf{E}}$ is a matrix in orbital subspace. Note that $\mathbf{A}_{\mathbf{E}}$ does not affect the heat-bath degrees of freedom because they are local and do not couple to the potential $\mathbf{A}_{\mathbf{E}}$.

The electric current density response, $\langle\mathbf{J}^e\rangle_{\mathbf{E}}$, due to $H'_{\mathbf{E}}$ can be computed similarly as $\langle\mathbf{J}^e\rangle_{\nabla\mu_F}$ in Appendix E:

$$\begin{aligned}\langle\mathbf{J}^e\rangle_{\mathbf{E}} &= q\frac{1}{i}\int\frac{d\mathbf{k}}{(2\pi)^2}\int\frac{d\omega}{2\pi}\mathrm{Tr}[\mathbf{v}G^<_{\mathbf{E}}]\\ &= q\int\frac{d\mathbf{k}}{(2\pi)^2}\int\frac{d\omega}{2\pi}\mathrm{Tr}\{\mathbf{v}[G_{\mathrm{R}}H'_{\mathbf{E}}G_{\mathrm{R}}\langle D^\dagger D\rangle G_{\mathrm{A}} + G_{\mathrm{R}}\langle D^\dagger D\rangle G_{\mathrm{A}}H'_{\mathbf{E}}G_{\mathrm{A}}]\}\\ &= -q^2\int\frac{d\mathbf{k}}{(2\pi)^2}\int\frac{d\omega}{2\pi}\mathrm{Tr}\{\mathbf{v}[G_{\mathrm{R}}v_j(\partial_\omega G^<) + G^<v_j(\partial_\omega G_{\mathrm{A}})]\}E_j\\ &= iq^2\int\frac{d\mathbf{k}}{(2\pi)^2}\int\frac{d\omega}{2\pi}\mathrm{Tr}\{\mathbf{v}[(\partial_\omega G_{\mathrm{R}})v_j\mathcal{A} - \mathcal{A}v_j(\partial_\omega G_{\mathrm{A}})]\}n_F E_j.\end{aligned} \tag{F2}$$

We have again used $t = -i\partial_\omega$, the fluctuation-dissipation relation Eq. (3.5), and the definition $G^< = (G_{\mathrm{A}} - G_{\mathrm{R}})n_F \equiv i\mathcal{A}n_F$ in Eq. (3.7). From Eq. (F2), we obtain

$$\sigma_{ij} = iq^2\frac{\epsilon_{zij}\epsilon_{zab}}{2}\int\frac{d\mathbf{k}}{(2\pi)^2}\int\frac{d\omega}{2\pi}\mathrm{Tr}[v_a(\partial_\omega G_{\mathrm{R}})v_b\mathcal{A} - v_a\mathcal{A}v_b(\partial_\omega G_{\mathrm{A}})]n_F. \tag{F3}$$

The antisymmetrization factor $\epsilon_{zij}\epsilon_{zab}/2$ is included since only the transverse part contributes to anomalous Hall transport. Equation (F3) is in the well-known Bastin form [53,64]. However, we emphasize that our Eq. (F3) has the inelastic self-energy naturally built in. One can also rewrite σ_{ij} in a Streda-like form [64] by splitting σ_{ij} into two halves and performing an integration by parts over ω on the second half, leading to $\mathcal{L}^{00}_{ij}$ in Eq. (2.2).

2. Derivation of γ_{xy}

Next we derive the anomalous γ_{xy} coefficient, which describes a heat-current response to the applied electric field. Unlike in the previous case, a calculation of γ_{xy} requires a proper subtraction of the charge magnetization current contribution [see

Eq. (2.1b)]. To derive γ_{xy}, we first calculate the "microscopic" heat current density due to the perturbation $H'_{\mathbf{E}}$, which follows closely that of $\langle \mathbf{J}^h \rangle_{\boldsymbol{\Theta}}$ in Sec. III B of the main text:

$$\begin{aligned}\langle \mathbf{J}^h \rangle_{\mathbf{E}} &= \frac{1}{i}\frac{1}{V}\int d\mathbf{x}dt \int d\mathbf{x}'dt' \mathrm{Tr}\left[\mathbf{v}(\mathbf{x}',\mathbf{x})\frac{i\partial_t - i\partial_{t'}}{2} G^<_{\mathbf{E}}(\mathbf{x}t,\mathbf{x}'t')\right] \\ &= \frac{1}{2}\int \frac{d\mathbf{k}}{(2\pi)^2}\int \frac{d\omega}{2\pi}\mathrm{Tr}\{\mathbf{v}\omega[G_{\mathrm{R}}H'_{\mathbf{E}}G_{\mathrm{R}}\langle D^\dagger D\rangle G_{\mathrm{A}} + G_{\mathrm{R}}\langle D^\dagger D\rangle G_{\mathrm{A}}H'_{\mathbf{E}}G_{\mathrm{A}}] \\ &\quad + \mathbf{v}[G_{\mathrm{R}}H'_{\mathbf{E}}G_{\mathrm{R}}\langle D^\dagger D\rangle \omega G_{\mathrm{A}} + G_{\mathrm{R}}\langle D^\dagger D\rangle G_{\mathrm{A}}H'_{\mathbf{E}}\omega G_{\mathrm{A}}]\} \\ &= -i\frac{q}{2}\int \frac{d\mathbf{k}}{(2\pi)^2}\int \frac{d\omega}{2\pi}\mathrm{Tr}\{\mathbf{v}\omega[G_{\mathrm{R}}v_j\partial_\omega(\mathcal{A}n_F) + \mathcal{A}n_F v_j\partial_\omega G_{\mathrm{A}}] - \mathbf{v}[(\partial_\omega G_{\mathrm{R}})v_j\omega\mathcal{A}n_F + [\partial_\omega(\mathcal{A}n_F)]v_j\omega G_{\mathrm{A}}]\}E_j. \end{aligned} \tag{F4}$$

This leads to $\langle J^h_i\rangle_{\mathbf{E}} = L^{h,e}_{ij}E_j$, with

$$L^{h,e}_{ij} = \frac{\epsilon_{zij}\epsilon_{zab}}{2}q\int\frac{d\mathbf{k}}{(2\pi)^2}\left\{\int\frac{d\omega}{2\pi}\mathrm{Tr}[v_aG_{\mathrm{R}}v_bG_{\mathrm{A}}]\omega(-\partial_\omega n_F) - \oint\frac{d\omega}{2\pi}\mathrm{Tr}[v_a(\partial_\omega G)v_bG]\omega n_F\right\}. \tag{F5}$$

According to Eq. (2.1), the transport thermoelectric coefficient γ_{ij} is given by

$$\gamma_{ij} = L^{h,e}_{ij} - \epsilon_{zji}M^e_z. \tag{F6}$$

Using Eq. (E5), for M^e_z, we immediately see that $\gamma_{ij} = \mathcal{L}^{10}_{ij}$ in Eq. (2.2) of the main text.

3. Derivation of β_{xy}

Now we present the derivation of the transport charge current response to an applied temperature gradient $\boldsymbol{\Theta} = -\boldsymbol{\nabla}T$. This derivation follows that of κ_{xy} in Sec. III B in large part. Without repeating the details, we note $\langle J^e_i\rangle_{\boldsymbol{\Theta}} \equiv L^{e,h}_{ij}(-\partial_j T)$ with $L^{e,h}_{ij}$ differing from that of $L^{h,h}_{ij}$ in Eq. (3.10) by a factor of q/ω, i.e.,

$$L^{e,h}_{ij} = -\frac{\epsilon_{zij}\epsilon_{zab}}{2}q\int\frac{d\mathbf{k}}{(2\pi)^2}\int\frac{d\omega}{2\pi}\mathrm{Tr}\left\{v_a\left[G_{\mathrm{R}}\frac{\partial\Sigma_{\mathrm{R}}}{\partial T}\partial_bG^< + G^<\frac{\partial\Sigma_{\mathrm{A}}}{\partial T}\partial_bG_{\mathrm{A}} + iG_{\mathrm{R}}\left(\frac{\partial}{\partial T}\langle D^\dagger D\rangle\right)\partial_bG_{\mathrm{A}}\right]\right\}. \tag{F7}$$

To obtain the transport β_{xy}, we again need to subtract the magnetization current contribution. From Eq. (2.1),

$$\beta_{ij} = L^{e,h}_{ij} - \epsilon_{izj}\frac{\partial M^e_z}{\partial T} \equiv \beta^{(1)}_{ij} + \beta^{(2)}_{ij}. \tag{F8}$$

As in Eq. (3.13), we divide β_{ij} into two pieces. $\beta^{(1)}_{ij}$ contains all contributions that involve $\partial\Sigma/\partial T$, while $\beta^{(2)}_{ij}$ contains the remainder. Now we show that, as a consequence of the fluctuation-dissipation relation, Eq. (3.5), $\beta^{(1)}_{ij} \equiv 0$. From Eq. (E5), we obtain

$$\frac{\partial M^e_z}{\partial T} = q\frac{\epsilon_{zij}}{2}\int\frac{d\mathbf{k}}{(2\pi)^2}\oint\frac{d\omega}{2\pi}\mathrm{Tr}\left\{\partial_\omega[v_i(\partial_TG)v_jG]\frac{1}{\beta}\mathrm{Li}_1(-e^{-\beta\omega}) + v_i(\partial_\omega G)v_jG[\mathrm{Li}_1(-e^{-\beta\omega}) - \beta\omega n_F]\right\}. \tag{F9}$$

In this equation, the first term depends on $\partial\Sigma/\partial T$ while the second does not. Using Eqs. (F7) and (F9) in Eq. (F8) and collecting all $\partial\Sigma/\partial T$ terms leads to

$$\begin{aligned}\beta^{(1)}_{ij} &= -\frac{\epsilon_{zij}\epsilon_{zab}}{2}\int\frac{d\mathbf{k}}{(2\pi)^2}\int\frac{d\omega}{2\pi}\mathrm{Tr}\left[v_aG_{\mathrm{R}}\frac{\partial\Sigma_{\mathrm{R}}}{\partial T}\partial_bG^< + v_aG^<\frac{\partial\Sigma_{\mathrm{A}}}{\partial T}\partial_bG_{\mathrm{A}} + v_aG_{\mathrm{R}}\frac{\partial(-2i\mathrm{Im}\Sigma)}{\partial T}\partial_bG_{\mathrm{A}}n_F\right] \\ &\quad + \frac{\epsilon_{zij}\epsilon_{zab}}{2}\int\frac{d\mathbf{k}}{(2\pi)^2}\oint\frac{d\omega}{2\pi}(\partial_\omega\mathrm{Tr}[v_a(\partial_TG)v_bG])\frac{1}{\beta}\mathrm{Li}_1(-e^{-\beta\omega}) \\ &= \frac{\epsilon_{zij}\epsilon_{zab}}{2}\int\frac{d\mathbf{k}}{(2\pi)^2}\oint\frac{d\omega}{2\pi}\left\{\mathrm{Tr}[v_a(\partial_TG)v_bG]n_F - \mathrm{Tr}[v_a(\partial_TG)v_bG]\partial_\omega\frac{1}{\beta}\mathrm{Li}_1(-e^{-\beta\omega})\right\} \\ &= 0. \end{aligned} \tag{F10}$$

To obtain the last line, we have used $\mathrm{Li}_1(x) = -\ln(1-x)$. Again, we emphasize that the fluctuation-dissipation relation in Eq. (3.5) is essential for the complete cancellation above. What remains in Eq. (F8) is then

$$\beta^{(2)}_{ij} = q\frac{\epsilon_{zij}\epsilon_{zab}}{2}\int\frac{d\mathbf{k}}{(2\pi)^2}\left\{\int\frac{d\omega}{2\pi}\mathrm{Tr}[v_aG_{\mathrm{R}}v_bG_{\mathrm{A}}]\left(-\frac{\omega}{T}\partial_\omega n_F\right) + \oint\frac{d\omega}{2\pi}\mathrm{Tr}[v_a(\partial_\omega G)v_bG][\mathrm{Li}_1(-e^{-\beta\omega}) - \beta\omega n_F]\right\}, \tag{F11}$$

which leads directly to $\mathcal{L}^{01}_{ij}$ in Eq. (2.2) of the main text.

APPENDIX G: CURRENT OPERATORS AND CONTINUITY EQUATIONS

In this Appendix, we define the charge and heat-current operators that we use to compute the transport coefficients and show they satisfy two continuity equations. We first define the charge and energy densities (ρ_i^e and ρ_i^h) at lattice site i from Eq. (3.1) as

$$\rho_i^e \equiv q\Big[\sum_m \psi_{im}^\dagger \psi_{im} + \sum_\alpha \phi_{i\alpha}^\dagger \phi_{i\alpha}\Big], \tag{G1a}$$

$$\rho_i^h \equiv \frac{1}{2}\sum_j \sum_{mn}[\psi_{im}^\dagger H_{im,jn}\psi_{jn} + \text{H.c.}] - \mu_F \sum_m \psi_{im}^\dagger \psi_{im} + \sum_\alpha a_\alpha \phi_{i\alpha}^\dagger \psi_{i\alpha} + \sum_{\alpha m}\eta_\alpha[\psi_{im}^\dagger \phi_{i\alpha} + \text{H.c.}]. \tag{G1b}$$

In the first term of ρ_i^h, the factor of $1/2$ is needed to avoid double counting so the total energy, i.e., the Hamiltonian, satisfies $H = \sum_i \rho_i^h$. For brevity, we have suppressed the time dependence of operators on both sides of these equations. Next we define the corresponding charge and heat-current density operators on the link that connects lattice site i and j as [65]

$$\mathbf{J}_{ij}^e \equiv \frac{q}{2i}\sum_{mn}[\psi_{im}^\dagger H_{im,jn}(\mathbf{x}_i - \mathbf{x}_j)\psi_{jn} - \text{H.c.}], \tag{G2a}$$

$$\mathbf{J}_{ij}^h \equiv \frac{1}{4}\sum_{mn}\{[\psi_{im}^\dagger H_{im,jn}(\mathbf{x}_i - \mathbf{x}_j)\dot{\psi}_{jn} - \dot{\psi}_{im}^\dagger H_{im,jn}(\mathbf{x}_i - \mathbf{x}_j)\psi_{jn}] + \text{H.c.}\}, \tag{G2b}$$

where $\dot{\psi}_{im} \equiv \partial_t \psi_{im}$ and $\mathbf{x}_i$ is the position of lattice site i. The heat-bath fermion field, $\phi_{i\alpha}$, does not enter the expressions of the charge and heat-current densities because it is local.

Using the following coupled EOM, derived from Eq. (3.1):

$$i\dot{\psi}_{im} = \sum_{jn} H_{im,jn}\psi_{jn} - \mu_F \psi_{im} + \sum_\alpha \eta_\alpha \phi_{i\alpha}, \tag{G3a}$$

$$i\dot{\phi}_{i\alpha} = a_\alpha \phi_{i\alpha} + \sum_m \eta_\alpha \psi_{im}, \tag{G3b}$$

one can easily prove that the following two continuity equations are satisfied:

$$\partial_t \rho_i^e + \sum_{j\neq i}\frac{(\mathbf{x}_j - \mathbf{x}_i)}{|\mathbf{x}_j - \mathbf{x}_i|^2}\cdot\left(2\mathbf{J}_{ij}^e\right) = 0, \tag{G4a}$$

$$\partial_t \rho_i^h + \sum_{j\neq i}\frac{(\mathbf{x}_j - \mathbf{x}_i)}{|\mathbf{x}_j - \mathbf{x}_i|^2}\cdot\left(2\mathbf{J}_{ij}^h\right) = 0. \tag{G4b}$$

These are the discretized form of the more familiar continuum equations, $\partial_t \rho^e + \nabla\cdot\mathbf{J}^e = 0$ and $\partial_t \rho^h + \nabla\cdot\mathbf{J}^h = 0$ [66]. The factor of 2 in $2\mathbf{J}_{ij}^e$ and $2\mathbf{J}_{ij}^h$ of Eq. (G4) appears because the total current along the link ij is given by $\mathbf{J}_{ij}^{e/h} + \mathbf{J}_{ji}^{e/h} = 2\mathbf{J}_{ij}^{e/h}$ [66].

In the main text, for convenience we have used a continuous notation for $\mathbf{J}^h$ in Eq. (3.8), which can be obtained from the discrete version in Eq. (G2b) by replacing $\{\psi_{im}^\dagger, -iH_{im,jn}(\mathbf{x}_i - \mathbf{x}_j), \psi_{jn}\}$ with $\{\psi^\dagger(\mathbf{x}'), \mathbf{v}(\mathbf{x}', \mathbf{x}), \psi(\mathbf{x}')\}$. Note that $\{\psi^\dagger(\mathbf{x}'), \mathbf{v}(\mathbf{x}', \mathbf{x}), \psi(\mathbf{x}')\}$ are either vectors or matrices in the orbital subspace.

[1] M. Banerjee, M. Heiblum, V. Umansky, D. E. Feldman, Y. Oreg, and A. Stern, Observation of half-integer thermal Hall conductance, Nature (London) **559**, 205 (2018).

[2] T. Qin, Q. Niu, and J. Shi, Energy Magnetization and the Thermal Hall Effect, Phys. Rev. Lett. **107**, 236601 (2011).

[3] D. Xiao, Y. Yao, Z. Fang, and Q. Niu, Berry-Phase Effect in Anomalous Thermoelectric Transport, Phys. Rev. Lett. **97**, 026603 (2006).

[4] C. L. Kane and M. P. A. Fisher, Quantized thermal transport in the fractional quantum Hall effect, Phys. Rev. B **55**, 15832 (1997).

[5] A. Cappelli, M. Huerta, and G. R. Zemba, Thermal transport in chiral conformal theories and hierarchical quantum Hall states, Nucl. Phys. B **636**, 568 (2002).

[6] M. Levin, B. I. Halperin, and B. Rosenow, Particle-Hole Symmetry and the Pfaffian State, Phys. Rev. Lett. **99**, 236806 (2007).

[7] S.-S. Lee, S. Ryu, C. Nayak, and M. P. A. Fisher, Particle-Hole Symmetry and the $\nu = \frac{5}{2}$ Quantum Hall State, Phys. Rev. Lett. **99**, 236807 (2007).

[8] D. Xiao, M.-C. Chang, and Q. Niu, Berry phase effects on electronic properties, Rev. Mod. Phys. **82**, 1959 (2010).

[9] N. Nagaosa, J. Sinova, S. Onoda, A. H. MacDonald, and N. P. Ong, Anomalous Hall effect, Rev. Mod. Phys. **82**, 1539 (2010).

[10] Y. Shiomi, Y. Onose, and Y. Tokura, Effect of scattering on intrinsic anomalous Hall effect investigated by Lorenz ratio, Phys. Rev. B **81**, 054414 (2010).

[11] X. Li, L. Xu, L. Ding, J. Wang, M. Shen, X. Lu, Z. Zhu, and K. Behnia, Anomalous Nernst and Righi-Leduc Effects in

Mn_3Sn: Berry Curvature and Entropy Flow, Phys. Rev. Lett. **119**, 056601 (2017).

[12] L. Xu, X. Li, X. Lu, C. Collignon, H. Fu, J. Koo, B. Fauque, B. Yan, Z. Zhu, and K. Behnia, Finite-temperature violation of the anomalous transverse wiedemann-franz law, Sci. Adv. **6**, eaaz3522 (2020).

[13] S. Onoda, N. Sugimoto, and N. Nagaosa, Quantum transport theory of anomalous electric, thermoelectric, and thermal Hall effects in ferromagnets, Phys. Rev. B **77**, 165103 (2008).

[14] X. Xu, J.-X. Yin, W. Ma, H.-R. Tian, X.-B. Qiang, P. V. S. Reddy, H. Zhou, J. Shen, H. Lu, T.-R. Chang, Z. Qu *et al.*, Topological charge-entropy scaling in kagome chern magnet $TbMn_6Sn_6$, Nat. Commun. **13**, 1197 (2022).

[15] A. O. Caldeira and A. J. Leggett, Path integral approach to quantum brownian motion, Physica A **121**, 587 (1983).

[16] J. M. Luttinger, Theory of thermal transport coefficients, Phys. Rev. **135**, A1505 (1964).

[17] R. C. Tolman, On the weight of heat and thermal equilibrium in general relativity, Phys. Rev. **35**, 904 (1930).

[18] A. Kapustin and L. Spodyneiko, Thermal Hall conductance and a relative topological invariant of gapped two-dimensional systems, Phys. Rev. B **101**, 045137 (2020).

[19] M. Stone, Gravitational anomalies and thermal Hall effect in topological insulators, Phys. Rev. B **85**, 184503 (2012).

[20] G. Tatara, Thermal Vector Potential Theory of Transport Induced by a Temperature Gradient, Phys. Rev. Lett. **114**, 196601 (2015).

[21] A. Gromov and A. G. Abanov, Thermal Hall Effect and Geometry with Torsion, Phys. Rev. Lett. **114**, 016802 (2015).

[22] A. Shitade, Heat transport as torsional responses and keldysh formalism in a curved spacetime, Prog. Theor. Exp. Phys. **2014**, 123I01 (2014).

[23] J. Park, O. Golan, Y. Vinkler-Aviv, and A. Rosch, Thermal Hall response: violation of gravitational analogues and einstein relations, arXiv:2108.06162.

[24] N. R. Cooper, B. I. Halperin, and I. M. Ruzin, Thermoelectric response of an interacting two-dimensional electron gas in a quantizing magnetic field, Phys. Rev. B **55**, 2344 (1997).

[25] We consider only orbital magnetizations in this paper and ignore any spin contributions.

[26] J. Shi, G. Vignale, D. Xiao, and Q. Niu, Quantum Theory of Orbital Magnetization and Its Generalization to Interacting Systems, Phys. Rev. Lett. **99**, 197202 (2007).

[27] R. Bianco and R. Resta, Orbital Magnetization as a Local Property, Phys. Rev. Lett. **110**, 087202 (2013).

[28] C. Xiao and Q. Niu, Unified bulk semiclassical theory for intrinsic thermal transport and magnetization currents, Phys. Rev. B **101**, 235430 (2020).

[29] For brevity, we will sometimes suppress the T dependence of Σ and show it explicitly only when necessary.

[30] Note that this cancellation is rather nontrivial for the transverse transport coefficients, as the appropriate charge and heat magnetization currents have to be properly included in the calculations.

[31] D. Groot and P. Mazur, *Non-Equilibrium Thermodynamics* (Dover Publications, New York, 1984)

[32] L. P. Kadanoff and G. Baym, *Quantum Statistical Mechanics: Green's Function Methods in Equilibrium and Nonequilibrium Problems*, edited by D. Pines (W. A. Benjamin, Inc., New York, 1962).

[33] A. Anisimov, W. Buchmuller, M. Drewes, and S. Mendizabal, Nonequilibrium dynamics of scalar fields in a thermal bath, Ann. Phys. **324**, 1234 (2009).

[34] C. Greiner and S. Leupold, Stochastic interpretation of kadanoff–baym equations and their relation to langevin processes, Ann. Phys. **270**, 328 (1998).

[35] See Ref. [67] and references therein for discussions in a different context.

[36] See Appendices for definitions of the tight-binding models, results of inelastic scattering effects on longitudinal transport coefficients and Wiedemann-Franz law, derivations of transport coefficients $\{\sigma_{xy}, \beta_{xy}, \gamma_{xy}\}$ as well as (charge and heat) orbital magnetizations, and a discussion of the continuity equations.

[37] The form of this spectrum is not important for our discussion.

[38] R. Kubo, The fluctuation-dissipation theorem, Rep. Prog. Phys. **29**, 255 (1966).

[39] In our convention, the time-frequency and space-momentum Fourier transformations are defined as $f(t) = \int \frac{d\omega}{2\pi} f(\omega) e^{-i\omega t}$ and $f(\mathbf{x}) = \int \frac{d\mathbf{k}}{(2\pi)^2} f(\mathbf{k}) e^{+i\mathbf{k}\cdot\mathbf{x}}$, respectively. For brevity, we also use the same notation for functions before and after the transformations.

[40] G. Mahan, *Many-Body Physics* (Kluwer Academic/Plenum Publishers, New York, 2000).

[41] This is because in the presence of a temperature gradient, to maintain a local equilibrium, the heat bath particle energy levels a_α needs to depend on the local temperature $T(\mathbf{x})$ at $\mathbf{x}$, leading to $a_\alpha \to a_\alpha - (\partial a_\alpha/\partial T)\mathbf{x}\cdot\boldsymbol{\Theta}$ in a linear expansion, which in turn leads to a shift in D_i and Σ.

[42] Note that, on the right-hand side, $\mathbf{x}$ is an operator which is nonlocal in $\mathbf{k}$ space and it is, therefore, important to keep track of its order with respect to other functions inside the expression. In Eq. (3.9), $\mathbf{x}$ operates on all functions to its right.

[43] We note that although defining the position operator $\mathbf{x}$ properly for a periodic lattice is subtle [57,68–70], within a gradient expansion due to a slowly varying external perturbation it is simply $i\nabla_{\mathbf{k}}$ in the $\mathbf{k}$ space. The subtlety does not come in here because the gradient expansion is a local one which does not depend on how one chooses the origin for $\mathbf{x}$ in spatial coordinates.

[44] T. Neupert, L. Santos, C. Chamon, and C. Mudry, Fractional Quantum Hall States at Zero Magnetic Field, Phys. Rev. Lett. **106**, 236804 (2011).

[45] Because electrons and phonons have different statistics and charge, this would require a modified treatment of our heat bath. However, to the extent that the dissipation we consider enters transport only through a local (i.e., $\mathbf{k}$ independent) electronic self-energy, we believe our formulas do not depend on the exact microscopic basis of Σ.

[46] A. Lavasani, D. Bulmash, and S. Das Sarma, Wiedemann-franz law and fermi liquids, Phys. Rev. B **99**, 085104 (2019).

[47] S. LaShell, E. Jensen, and T. Balasubramanian, Nonquasiparticle structure in the photoemission spectra from the Be(0001) surface and determination of the electron self energy, Phys. Rev. B **61**, 2371 (2000).

[48] We have also checked that this enhancement occurs in all the models we have studied, including different variants of H_{II}, and we believe that it is universal.

[49] L. Ding, J. Koo, L. Xu, X. Li, X. Lu, L. Zhao, Q. Wang, Q. Yin, H. Lei, B. Yan, Z. Zhu, and K. Behnia, Intrinsic Anomalous Nernst Effect Amplified by Disorder in a Half-Metallic Semimetal, Phys. Rev. X **9**, 041061 (2019).

[50] R. Nourafkan and A. M. S. Tremblay, Hall and faraday effects in interacting multiband systems with arbitrary band topology and spin-orbit coupling, Phys. Rev. B **98**, 165130 (2018).

[51] G. Sharma, P. Goswami, and S. Tewari, Nernst and magnetothermal conductivity in a lattice model of weyl fermions, Phys. Rev. B **93**, 035116 (2016).

[52] L. Smrcka and P. Streda, Transport coefficients in strong magnetic fields, J. Phys. C: Solid State Phys. **10**, 2153 (1977).

[53] A. Bastin, C. Lewiner, O. Betbeder-matibet, and P. Nozieres, Quantum oscillations of the Hall effect of a fermion gas with random impurity scattering, J. Phys. Chem. Solids **32**, 1811 (1971).

[54] V. P. Gusynin, S. G. Sharapov, and A. A. Varlamov, Anomalous thermospin effect in the low-buckled dirac materials, Phys. Rev. B **90**, 155107 (2014).

[55] R. Matsumoto, R. Shindou, and S. Murakami, Thermal Hall effect of magnons in magnets with dipolar interaction, Phys. Rev. B **89**, 054420 (2014).

[56] D. Ceresoli, T. Thonhauser, D. Vanderbilt, and R. Resta, Orbital magnetization in crystalline solids: multi-band insulators, chern insulators, and metals, Phys. Rev. B **74**, 024408 (2006).

[57] R. Resta, Electrical Polarization and Orbital Magnetization: The Position Operator Tamed, in *Handbook of Materials Modeling: Methods: Theory and Modeling*, edited by W. Andreoni and S. Yip (Springer International Publishing, Cham, 2018), pp. 1–31.

[58] H. Kontani, T. Tanaka, and K. Yamada, Intrinsic anomalous Hall effect in ferromagnetic metals studied by the multi-*d*-orbital tight-binding model, Phys. Rev. B **75**, 184416 (2007).

[59] Z. Wang, G. Chaudhary, Q. Chen, and K. Levin, Quantum geometric contributions to the bkt transition: Beyond mean field theory, Phys. Rev. B **102**, 184504 (2020).

[60] J. S. Hofmann, E. Berg, and D. Chowdhury, Superconductivity, pseudogap, and phase separation in topological flat bands, Phys. Rev. B **102**, 201112(R) (2020).

[61] L. Zhang, Berry curvature and various thermal Hall effects, New J. Phys. **18**, 103039 (2016).

[62] A. Kapustin and L. Spodyneiko, Microscopic formulas for thermoelectric transport coefficients in lattice systems, Phys. Rev. B **104**, 035150 (2021).

[63] S. Tan and K. Levin, Nernst effect and anomalous transport in cuprates: A preformed-pair alternative to the vortex scenario, Phys. Rev. B **69**, 064510 (2004).

[64] A. Crépieux and P. Bruno, Theory of the anomalous Hall effect from the kubo formula and the dirac equation, Phys. Rev. B **64**, 014416 (2001).

[65] I. Paul and G. Kotliar, Thermal transport for many-body tight-binding models, Phys. Rev. B **67**, 115131 (2003).

[66] T. B. Boykin, M. Luisier, and G. Klimeck, Current density and continuity in discretized models, Eur. J. Phys. **31**, 1077 (2010).

[67] R. Boyack, Z. Wang, Q. Chen, and K. Levin, Unified approach to electrical and thermal transport in high-T_c superconductors, Phys. Rev. B **104**, 064508 (2021).

[68] E. I. Blount, *Solid State Physics: Advanced in Research and Applications*, edited by F. Seitz and D. Turnbull (Academic, New York, 1962), Vol. 13.

[69] G. B. Ventura, D. J. Passos, J. M. B. Lopes dos Santos, J. M. Viana Parente Lopes, and N. M. R. Peres, Gauge covariances and nonlinear optical responses, Phys. Rev. B **96**, 035431 (2017).

[70] D. E. Parker, T. Morimoto, J. Orenstein, and J. E. Moore, Diagrammatic approach to nonlinear optical response with application to weyl semimetals, Phys. Rev. B **99**, 045121 (2019).